funding

The study was not supported by a sponsor or funding agency.

disclosure

The authors declare no conflicts of interest.

references

1. Breathnach OS, Freidlin B, Conley B et al. Twenty-two years of phase III trials for patients with advanced non-small-cell lung cancer: sobering results. J Clin Oncol 2001; 19: 1734–1742.
2. Carney DN. Lung cancer—time to move on from chemotherapy. N Engl J Med 2002; 346: 126–128.
3. Hotta K, Matsuo K. Long-standing debate on cisplatin- versus carboplatin-based chemotherapy in the treatment of advanced non-small cell lung cancer. J Thorac Oncol 2007; 2: 96.
4. Hotta K, Matsuo K, Ueoka H et al. Meta-analysis of randomized clinical trials comparing cisplatin to carboplatin in patients with advanced non-small-cell lung cancer. J Clin Oncol 2004; 22: 3852–3859.
5. Azzoli CG, Baker S Jr, Temin S et al. American Society of Clinical Oncology Clinical Practice Guideline update on chemotherapy for stage IV non-small-cell lung cancer. J Clin Oncol 2009; 27: 6251–6266.
6. Wakelee HA, Bernardo P, Johnson DH, Schiller JH. Changes in the natural history of nonsmall cell lung cancer (NSCLC)—comparison of outcomes and characteristics in patients with advanced NSCLC entered in Eastern Cooperative Oncology Group trials before and after 1990. Cancer 2006; 106: 2208–2217.
7. Soria JC, Massard C, Le Chevalier T. Should progression-free survival be the primary measure of efficacy for advanced NSCLC therapy? Ann Oncol 2010; 21: 2324–2332.
8. Reck M, von Pawel J, Zatloukal P et al. Overall survival with cisplatin-gemcitabine and bevacizumab or placebo as first-line therapy for nonsquamous non-small-cell lung cancer: results from a randomised phase III trial (AVAiL). Ann Oncol 2010; 21: 1804–1809.
9. Reck M, von Pawel J, Zatloukal P et al. Phase III trial of cisplatin plus gemcitabine with either placebo or bevacizumab as first-line therapy for nonsquamous non-small-cell lung cancer: AVAil. J Clin Oncol 2009; 27: 1227–1234.
10. Saad ED, Katz A, Buyse M. Overall survival and post-progression survival in advanced breast cancer: a review of recent randomized clinical trials. J Clin Oncol 2010; 28: 1958–1962.
11. DerSimonian R, Laird N. Meta-analysis in clinical trials. Control Clin Trials 1986; 7: 177–188.
12. Broglio KR, Berry DA. Detecting an overall survival benefit that is derived from progression-free survival. J Natl Cancer Inst 2009; 101: 1642–1649.
13. Sandler AB, Nemunaitis J, Denham C et al. Phase III trial of gemcitabine plus cisplatin versus cisplatin alone in patients with locally advanced or metastatic non-small-cell lung cancer. J Clin Oncol 2000; 18: 122–130.
14. Fossella FV, DeVore R, Kerr RN et al. Randomized phase III trial of docetaxel versus vinorelbine or ifosfamide in patients with advanced non-small-cell lung cancer previously treated with platinum-containing chemotherapy regimens. The TAX 320 Non-Small Cell Lung Cancer Study Group. J Clin Oncol 2000; 18: 2354–2362.
15. Hanna N, Shepherd FA, Fossella FV et al. Randomized phase III trial of pemetrexed versus docetaxel in patients with non-small-cell lung cancer previously treated with chemotherapy. J Clin Oncol 2004; 22: 1589–1597.
16. Kim ES, Hirsh V, Mok T et al. Gefitinib versus docetaxel in previously treated non-small-cell lung cancer (INTEREST): a randomised phase III trial. Lancet 2008; 372: 1809–1818.
17. Shepherd FA, Rodrigues Pereira J, Ciuleanu T et al. Erlotinib in previously treated non-small-cell lung cancer. N Engl J Med 2005; 353: 123–132.
18. Buyse M, Squifflet P, Laporte S et al. Prediction of survival benefits from progression-free survival in patients with advanced non small cell lung cancer: evidence from a pooled analysis of 2,838 patients randomized in 7 trials. J Clin Oncol 2008; 26 (Suppl): (Abstr 8019).
19. Mauguen A, Michiels S, Burdett S et al. Evaluation of progression-free survival as a surrogate endpoint for overall survival when evaluating the effect of chemotherapy and radiotherapy in locally advanced lung cancer using data from four individual patient data meta-analyses. J Thorac Oncol 2011; 6 (Suppl 2): S464–S465.
20. Hotta K, Fujiwara Y, Matsuo K et al. Time to progression as a surrogate marker for overall survival in patients with advanced non-small cell lung cancer. J Thorac Oncol 2009; 4: 311–317.
21. Johnson KR, Ringland C, Stokes BJ et al. Response rate or time to progression as predictors of survival in trials of metastatic colorectal cancer or non-small-cell lung cancer: a meta-analysis. Lancet Oncol 2006; 7: 741–746.

Annals of Oncology

Annals of Oncology 24: 84–90, 2013
doi:10.1093/annonc/mds215
Published online 10 August 2012

Diagnostic and prognostic significance of the alternatively spliced *ACTN4* variant in high-grade neuroendocrine pulmonary tumours

A. Miyanaga[1,2], K. Honda[1], K. Tsuta[3], M. Masuda[1], U. Yamaguchi[1], G. Fujii[4], A. Miyamoto[5], S. Shinagawa[5], N. Miura[1], H. Tsuda[3], T. Sakuma[6], H. Asamura[7], A. Gemma[2] & T. Yamada[1]*

[1]*Division of Chemotherapy and Clinical Research, National Cancer Center Research Institute, Tokyo;* [2]*Department of Internal Medicine, Division of Pulmonary Medicine, Infection and Oncology, Nippon Medical School, Tokyo;* [3]*Division of Pathology and Clinical Laboratories, National Cancer Center Hospital, Tokyo;* [4]*Division of Cancer Prevention Research, National Cancer Center Research Institute, Tokyo ;* [5]*Kobe Research Center, TransGenic Inc., Kumamoto;* [6]*BioBusiness Group, Mitsui Knowledge Industry, Tokyo;* [7]*Division of Thoracic Surgery, National Cancer Center Hospital, Tokyo, Japan*

Received 2 April 2012; revised 30 May 2012; accepted 31 May 2012

Background: High-grade neuroendocrine tumours (HGNTs) of the lung manifest a wide spectrum of clinical behaviour, but no method for predicting their outcome has been established.
Materials and methods: We newly established a monoclonal antibody specifically recognizing the product of the alternatively spliced *ACTN4* transcript (namely, variant actinin-4), and used it to examine the expression of variant actinin-4 immunohistochemically in a total of 609 surgical specimens of various histological subtypes of lung cancer.
Results: Variant actinin-4 was expressed in 55% (96/176) of HGNTs, but in only 0.8% (3/378) of non-neuroendocrine (NE) lung cancers. The expression of variant actinin-4 was significantly associated with poorer overall survival in HGNT patients ($P = 0.00021$, log-rank test). Multivariate analysis using the Cox proportional hazards model showed that the expression of variant actinin-4 was the most significant independent negative predictor of survival in HGNT patients (hazard ratio (HR), 2.15; $P = 0.00113$) after the presence of lymph node metastasis (HR, 2.25; $P = 0.00023$).
Conclusions: The expression of variant actinin-4 is an independent prognostic factor for patients with HGNTs. This protein has a high affinity for filamentous actin polymers and likely promotes aggressive behaviour of cancer cells. The present clinical findings clearly support this notion.
Key words: actinin-4, alternative splice variant, diagnostic marker, high-grade neuroendocrine tumour, pulmonary neoplasm, prognosis

introduction

Neuroendocrine (NE) tumours comprise 20%–25% of all human lung malignancies and are classified into four histological subtypes: typical carcinoid (TC), atypical carcinoid (AC), large cell neuroendocrine carcinoma (LCNEC) and small cell lung carcinoma (SCLC) [1, 2]. TC and AC are tumours with low- to intermediate-grade malignancy, whereas LCNEC and SCLC are highly aggressive and collectively referred to as high-grade neuroendocrine tumours (HGNTs) [3–6].

LCNEC appeared in the World Health Organization (WHO) Histological Typing of Lung and Pleural Tumours (third version, 1999) as a new entity of large cell carcinoma [2]. LCNEC shows aggressive behaviour distinct from other non-small cell lung cancers (NSCLCs) [7], and thus its accurate discrimination is essential for the management of lung cancer patients. TC, AC and SCLC can be readily diagnosed on the basis of their histological characteristics, but the diagnosis of LCNEC is more complicated. The morphological features of NE differentiation are often inconspicuous, especially in small biopsy or cytology specimens [2].

Three NE markers are used routinely for immunohistochemical assessment of NE differentiation: neural cell adhesion molecule (CD56), chromogranin A (CGA) and synaptophysin (SYN). However, a significant proportion of LCNECs are negative for any of these NE markers [7], and more problematically, some non-NE lung cancers also show equivocal immunoreactivity for these markers [7, 8]. Therefore, it is necessary to develop a new diagnostic biomarker with higher specificity.

Actinin-4 is an actin-binding protein that we originally identified as being associated with enhanced cell motility and cancer invasion [9]. The actinin-4 (*ACTN4*) gene has a unique structure (supplementary Figure S1, available at *Annals of*

Correspondence to: Prof. T. Yamada, Division of Chemotherapy and Clinical Research, National Cancer Center Research Institute, 5-1-1 Tsukiji, Chuo-ku, Tokyo 104-0045, Japan. Tel: +81-3-3542-2511; Fax: +81-3-3547-6045; E-mail: tyamada@ncc.go.jp

Oncology online), possessing two exons 8 (8 and 8[?]) of the same size, the mutually exclusive use of which leads to the production of two kinds of mRNA. The transcript obtained with exon 8 is expressed ubiquitously (namely, the ubiquitous form or *ACTN4*-Ub), whereas the expression of the variant transcript obtained with exon 8[?] (the variant form or *ACTN4*-Va) is undetectable in normal tissues except for testis and brain [10, 11]. We previously found that the variant transcript is frequently expressed in SCLCs and that the gene product can be categorized as a so-called cancer-testis antigen [10]. However, the clinical significance of variant actinin-4 has remained undetermined due to lack of a specific probe.

The alternatively spliced actinin-4 variant transcript is predicted to encode a polypeptide differing in only three amino acids. To produce an antibody that can detect this small difference, we used the *GANP* (germinal centre-associated nuclear protein) technology [12]. *GANP* transgenic mice generate a highly diverse spectrum of antibodies and have been used to produce high-affinity antibodies against various difficult antigens, such as those with small protein modifications [13]. Here, we report the establishment of a highly specific antibody recognizing variant actinin-4 protein and the potential utility of variant actinin-4 not only as a new diagnostic biomarker but also as a highly potent prognostic biomarker for HGNTs.

materials and methods

cell lines and sequencing

Total RNA was extracted from 91 human cancer cell lines (31 lung cancers, 23 colorectal cancers, 7 stomach cancers, 5 hepatocellular carcinomas, 6 pancreatic cancers, 4 choriocarcinomas, 4 ovary cancers, 4 oral cancers, 3 prostate cancers, 2 breast cancers, 1 bladder cancer and 1 cervical cancer) using TRIzol reagent (Life Technologies, Grand Island, NY) (supplementary Table S1, available at *Annals of Oncology* online).

First-strand complementary DNA (cDNA) was synthesized in the presence of random primers using the high-capacity cDNA reverse transcription kit (Life Technologies) in accordance with the manufacturer's instructions. The entire coding region of *ACTN4* was amplified and sequenced using the BigDye Terminator v3.1 Cycle Sequencing Ready Reaction Kit (Life Technologies).

production of monoclonal antibodies

GANP transgenic mice were immunized with a synthetic peptide (NQSYQYGPSSAGNGAG) to produce a monoclonal antibody (namely 13G9) reactive with all the known forms (ubiquitous and variant) of actinin-4. Another monoclonal antibody specific to variant actinin-4 (namely 15H2) was raised against a synthetic peptide (DIVGTLRPDEKAIMTYVSC). The reactivity and titre of antibodies against the various peptides were assessed by the antibody capture assay as described previously [13].

western blot analysis

The PCR-amplified fragments encoding the ubiquitous and variant forms of actinin-4 (amino acids 28–911) were cloned into the EcoRI and KpnI sites of the pEGFP-C1 vector (Takara Bio, Otsu, Japan) to express the ubiquitous and variant actinin-4 proteins fused with green fluorescent protein (GFP) at the N-termini (namely pEGFP-ACTN4-Ub and pEGFP-ACTN4-Va, respectively). The nucleotide sequences of all the PCR-amplified fragments were verified by sequencing. HEK293 cells (Health Science Research Resources Bank, Osaka, Japan) were transfected with each plasmid using Lipofectamine 2000 reagent (Life Technologies).

Western blotting was carried out following standard procedures, as described previously [14, 15]. Cells were extracted with lysis buffer [10 mmol/l HEPES (pH 7.4), 150 mmol/l NaCl, 1 mmol/l EDTA, 1% Triton X-100, 1% NP40 and 1 mg/ml NaN_3] containing a protease inhibitor cocktail (Sigma-Aldrich, St. Louis, MO) on ice for 30 min. Ten micrograms of cell lysate were reduced, denatured at 70°C for 10 min and fractionated through NuPAGE 4%–12% Bis-Tris gel (Life Technologies). The fractionated proteins were then blotted onto PVDF membranes (Life Technologies). After incubation with the primary antibody at 4°C overnight, the blots were incubated with appropriate horseradish peroxidase-linked secondary antibodies and then detected by enhanced chemiluminescence (Western Lightning ECL Pro; Perkin-Elmer, Waltham, MA).

patients and tissue samples

Thirty-one tissue microarrays (TMAs) were constructed from formalin-fixed paraffin-embedded tissue blocks of 609 primary lung tumours that had been surgically resected at the National Cancer Center (NCC) Hospital (Tokyo, Japan) from 1982 to 2010 using a tissue-arraying instrument (KIN-1; Azumaya, Tokyo, Japan). Based on the Pathology and genetics of Tumours of the Lung, Pleura, Thymus and Heart [IARC (International Agency for Research on Cancer) WHO Classification of Tumours] (2004) [16], the 609 tumours were classified into carcinoid (51 cases), SCLC (70 cases), LCNEC (106 cases), adenocarcinoma (164 cases), squamous cell carcinoma (166 cases) and other NSCLCs (52 cases). To reduce sampling bias due to tissue heterogeneity, we took duplicate core samples measuring 2.0 mm in diameter from two different areas of every tumour.

The 176 patients with HGNTs included 143 men and 33 women with a mean age of 66 years (19–84 years). One hundred and sixty-nine (96%) patients had a history of habitual cigarette smoking. The follow-up periods ranged from 1 to 286 months (median follow-up, 46 months). Patients were staged postsurgically into IA (52 cases), IB (25 cases), IIA (33 cases), IIB (16 cases), IIIA (37 cases), IIIB (7 cases) and IV (6 cases) according to the International Union against Cancer (UICC) TNM classification of malignant tumours (7th edition, 2010) [17].

This study was conducted with approval from the Institutional Review Board of the NCC.

immunohistochemistry

TMA blocks were then cut into 4-mm thick sections and subjected to immunohistochemistry (IHC). Immunostaining of actinin-4 proteins was carried out using the Ventana DABMap detection kit and an automated slide stainer (Discovery XT, Ventana Medical Systems, Tucson, AZ) [18, 19]. Immunoreactivity was classified as positive when ≥10% of cancer cells showed cytoplasmic or membrane staining detectable at a magnification of ×40 [20, 21].

Deparaffinized TMA slides were incubated with anti-CD56 mouse monoclonal (1B6, Novocastra, Newcastle upon Tyne, UK), anti-CGA rabbit polyclonal (Dako, Glostrup, Denmark) or anti-SYN mouse monoclonal (27G12, Nichirei Biosciences, Tokyo, Japan) antibody for 1 h at room temperature. Immunoreactivity was detected with the EnVision plus kit (Dako) using 3, 3[?]-diaminobenzidine as the chromogen. For diagnosis of LCNEC, positive staining for at least one of the three NE markers was stipulated.

The results of IHC were judged by two investigators (AM and KT) who were blinded to any clinicopathological information, and any discrepancy in judgement was discussed.

statistical analysis

Overall survival was measured as the period from surgery to the date of death or last follow-up. Progression-free survival was defined as the length of time from surgery to the first detection of new lesions or death. Overall and progression-free survival was estimated by the Kaplan–Meier method using the StatFlex statistical software package (version 5.0, Artiteck, Osaka, Japan). Differences between the survival curves were assessed with the log-rank test. Univariate and multivariate analyses were carried out using the Cox regression model. Other statistical tests were carried out using tools available in the R statistical package (version 2.12.0; http://www.r-project.org/). Differences were considered to be statistically significant at $P < 0.05$.

results

expression of the *ACTN4* splice variant in cancer cell lines

We sequenced the entire coding region of the *ACTN4* transcript in 91 cell lines derived from human cancers of various origins (supplementary Table S1, available at *Annals of Oncology* online). No non-synonymous nucleotide substitution was detected except for those registered in the single nucleotide polymorphism database (http://www.ncbi.nlm.nih.gov/snp), indicating that somatic mutation of the *ACTN4* gene is infrequent. However, we detected overlap of two sequences appearing in nucleotides 793–872 of the *ACTN4* transcript (NM_004924.2) (supplementary Figure S2A, available at *Annals of Oncology* online) in 25% (23/91) of the cell lines. These two transcripts were separately cloned, and their nucleotide sequences were confirmed to be identical to the ubiquitous and variant transcripts of *ACTN4* that we had described previously [10] (supplementary Figure S2B, available at *Annals of Oncology* online).

The ubiquitous form of the *ACTN4* transcript (namely *ACTN4*-Ub) was expressed in all of the 91 human cancer cell lines examined, but the variant form (namely *ACTN4*-Va) was detected in 90% (18/20) of the SCLC cell lines examined (SBC-3, SBC-5, MS-1-L, Lu-135, Lu-143, STC-1, Lu-138, Lu-140, DMS153, DMS53, H1688, Wa-hT, H69AR, RERF-LCMS, Lu165, H69, Lu134-AH, Lu134-B, Lu-141 and Lu-139) and 25% (1/4) of the cell lines derived from pulmonary carcinoid tumour (NCI-H727, NCI-H835, UMC-11 and NCI-H720) (supplementary Table S1, available at *Annals of Oncology* online). In addition, the variant *ACTN4* mRNA was detected in 33% (1/3) of prostate cancers and 75% (3/4) of choriocarcinoma cell lines. However, none of the seven non-SCLC-derived cell lines examined (A549, PC9, LCD, LCKJ, LK-2, Lu-65 and Lu-99) expressed the variant transcript.

production of antibody specific to variant actinin-4 protein

Although there was a difference of only three amino acid residues between the ubiquitous and variant actinin-4 protein sequences deduced from their cDNA sequences (supplementary Figure S2C, available at *Annals of Oncology* online), we were able to produce a monoclonal antibody (15H2) that reacted specifically with a peptide for which the amino acid sequence was derived from the variant actinin-4 protein (DIVGTLRPDEKAIMTYVSC), but not with the corresponding sequence of the ubiquitous protein (DIVNTARPDEKAIMTYVSS) (underlining indicates the amino acids that differed) (Figure 1A).

To further confirm that the 15H2 monoclonal antibody reacted specifically with the variant form of actinin-4 protein, HEK 293 cells were transfected with a plasmid encoding the ubiquitous (pEGFP-ACTN4-Ub) or variant (pEGFP-ACTN4-Va) form of actinin-4. We found that the 15H2 antibody reacted only with a lysate prepared from HEK 293 cells transfected with pEGFP-ACTN4-Va, but not with those prepared from cells transfected with pEGFP-ACTN4-Ub or the parental pEGFP-C1 vector (ACTN4-Va, Figure 1B). On the other hand, the monoclonal antibody 13G9 reacted with both the ubiquitous and variant actinin-4 proteins (pan-ACTN4, Figure 1B).

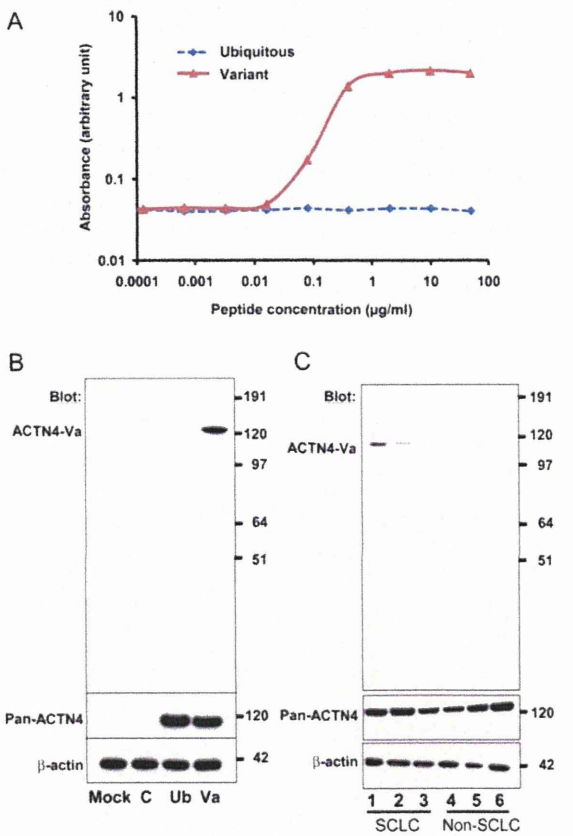

Figure 1. Specificity of the 15H2 monoclonal antibody to the actinin-4 variant. (A) Reactivity of the 15H2 monoclonal antibody with the synthetic peptides DIVNTARPDEKAIMTYVSS (ubiquitous) and DIVGTLRPDEKAIMTYVSC (variant), as determined by the antibody capture assay. (B) Proteins were extracted from HEK293 cells that had been transfected with no plasmid (mock), pEGFP (C), pEGFP-ACTN4-Ub (Ub) or pEGFP-ACTN4-Va (Va) and blotted with 15H2 (ACTN4-Va), 13G9 (pan-ACTN4) and anti-β-actin (loading control) antibodies. Molecular masses (in kiloDaltons) are shown on the right. (C) Proteins were extracted from three small cell lung carcinoma (SCLC) cell lines [SBC3- (lane 1), Lu-135 (2) and Lu-165 (3)] and three non-small cell lung carcinoma (NSCLC) cell lines [LCD (4), LK-2 (5) and EBC-1 (6)] and blotted with 15H2 (ACTN4-Va), 13G9 (pan-ACTN4) and anti-β-actin (loading control) antibodies. Molecular masses (in kiloDaltons) are shown on the right.

The expression of endogenous variant actinin-4 was detected in all three SCLC cell lines examined (SBC-3, Lu-135 and Lu-165), but in none of the three non-SCLC cell lines (LCD, LK-2 and EBC-1) (Figure 1C), being consistent with the results of cDNA sequencing described above.

significance of variant actinin-4 expression in the diagnosis of HGNT

We next investigated immunohistochemically the expression of both actinin-4 proteins and classical NE markers (CGA, SYN and CD56) in 609 primary lung tumours. Representative results of immunohistochemical staining are shown in Figure 2, and the positivity rates for each histological subtype are summarized in Table 1. CGA was expressed in 88% (59/67) of SCLCs and 56% (59/105) of LCNECs. SYN was expressed in 88% (58/66) of SCLCs and 56% (59/105) of LCNECs. CD56 was expressed in 96% (64/67) of SCLCs and 72% (76/105) of LCNECs. The three NE markers were also expressed in 76%–100% of pulmonary carcinoid tumours (Table 1). The expression of variant actinin-4 protein was detected in 55% (96/176) of HGNTs [60% (42/70) of SCLCs and 51% (54/106) of LCNECs], but in only 10% (5/51) of carcinoid tumours. The difference in the frequency of variant actinin-4 expression between HGNTs and carcinoid tumours was statistically significant ($P = 6.0 \times 10^{-6}$, Fisher's exact test).

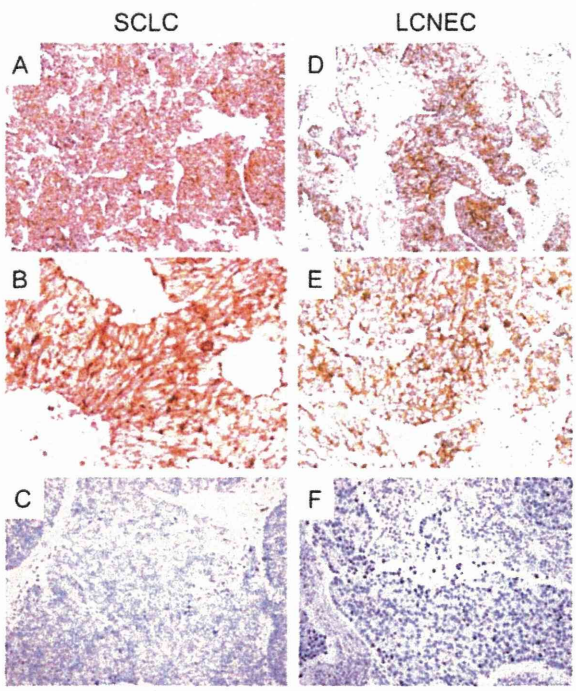

Figure 2. Expression of the variant actinin-4 protein in high-grade neuroendocrine tumour (HGNT). Representative cases of small cell lung carcinoma (SCLC) (A–C) and large cell neuroendocrine carcinoma (LCNEC) (D–F) showing positive (A, B, D and E) and negative (C and F) immunoreactivity with the 15H2 monoclonal antibody. Original magnification: A, C, D and F, ×20; B and E, ×400.

CGA, SYN and CD56 were found to show variable expression in non-NE lung tumours (2%–11% of adenocarcinomas, 2%–14% of squamous cell carcinomas and 6%–17% of other NSCLCs). However, variant actinin-4 protein was expressed in only 0.8% (3/382) of non-NE NSCLCs. These results indicated that variant actinin-4 was highly specific to HGNTs.

prognostic significance of variant actinin-4 expression

There was no significant difference between patients with HGNTs that were positive ($n = 96$) and negative ($n = 80$) for variant actinin-4 protein expression with respect to gender, age, smoking status, histological subtype (LCNEC versus SCLC), pathological stage, tumour size or frequency of lymph node or distant metastasis (Table 2). However, the frequency of relapse after surgery was much higher in stage I to III HGNT cases that were positive for variant actinin-4 protein expression [67% (53/79)] than in cases that were negative [43% (39/91)] ($P = 0.0020$, Fisher's exact test) (Table 2). The sites of first recurrence in patients with HGNTs that were positive for variant actinin-4 expression included the brain (16 cases), lymph nodes (16 cases), lung (9 cases), liver (6 cases), and bone (5 cases), but the site distribution did not differ significantly from that in negative cases.

The overall survival of patients with variant actinin-4-positive HGNT, SCLC and LCNEC was significantly worse than that of patients whose tumours were negative [$P = 0.00021$ (HGNT, Figure 3A), 0.0283 (SCLC, supplementary Figure S3A, available at *Annals of Oncology* online) and 0.0022 (LCNEC, supplementary Figure S3B, available at *Annals of Oncology* online), log-rank test]. Furthermore, progression-free survival also differed significantly between patients whose tumours were positive and negative for variant actinin-4 expression [$P = 0.0021$ (HGNT, Figure 3B), 0.018 (SCLC, supplementary Figure S3C, available at *Annals of Oncology* online) and 0.048 (LCNEC, supplementary Figure S3D, available at *Annals of Oncology* online), log-rank test]. The 5-year survival rates of patients with variant actinin-4-negative HGNT, SCLC and LCNEC were 62%, 62% and 62%, respectively, whereas those of

Table 1. Expression of variant actinin-4 and three NE markers in various histological subtypes of lung cancer

Histological subtype[a]	*N*	Variant actinin-4	CGA	SYN	CD56
SCLC	70	42 (60%)	59 (88%)	58 (88%)	64 (96%)
LCNEC	106	54 (51%)	59 (56%)	59 (56%)	76 (72%)
Carcinoid	51	5 (10%)	49 (100%)	49 (100%)	37 (76%)
Adenocarcinoma	164	1 (1%)	16 (11%)	6 (4%)	4 (2%)
Squamous cell carcinoma	166	2 (1%)	23 (14%)	4 (2%)	16 (10%)
Others	52	0 (0%)	9 (17%)	5 (10%)	3 (6%)

SCLC, small cell lung carcinoma; LCNEC, large cell neuroendocrine carcinoma; NE, neuroendocrine; CGA, chromogranin A; SYN, synaptophysin; IARC, International Agency for Research on Cancer; WHO, World Health Organization.

[a]Based on the Pathology and Genetics of Tumours of the Lung, Thymus and Heart (IARC WHO Classification of tumours) (third version, 2004).

Table 2. Association of expression of the actinin-4 variant with clinicopathological characteristics of high-grade neuroendocrine tumour (HGNT) patients

Characteristic		Actinin-4 splice variant		*P* value[a]
	Total	Positive (%)	Negative (%)	
Sex				
Male	143	78 (55%)	65 (46%)	1
Female	33	18 (55%)	15 (46%)	
Age				
≥65 years	105	60 (57%)	45 (43%)	0.442
<65 years	71	36 (51%)	35 (49%)	
Smoking status				
Never smoked	7	3 (43%)	4 (57%)	0.703
Current or former smoker	169	93 (55%)	76 (45%)	
Histological subtype				
SCLC	70	42 (60%)	28 (40%)	0.280
LCNEC	106	54 (51%)	52 (49%)	
Pathological stage[b]				
I, II	124	62 (50%)	62 (50%)	0.069
III, IV	52	34 (65%)	18 (35%)	
Tumour size				
≤3 cm	94	56 (60%)	38 (40%)	0.173
>3 cm	82	40 (49%)	42 (51%)	
Lymph node metastasis				
Absent	101	50 (50%)	51 (51%)	0.129
Present	75	46 (61%)	29 (39%)	
Distant metastasis				
Absent	170	92 (54%)	78 (46%)	0.690
Present	6	4 (67%)	2 (33%)	
Recurrence				
Absent	91	39 (43%)	52 (57%)	**0.00200**
Present	79	53 (67%)	26 (33%)	

SCLC, small cell lung carcinoma; LCNEC, large cell neuroendocrine carcinoma.

[a]Fisher's exact test. *P* values of < 0.05 are shown in bold.

[b]According to the International Union Against Cancer (UICC) TNM Classification of Malignant Tumours, 7th edition (2010).

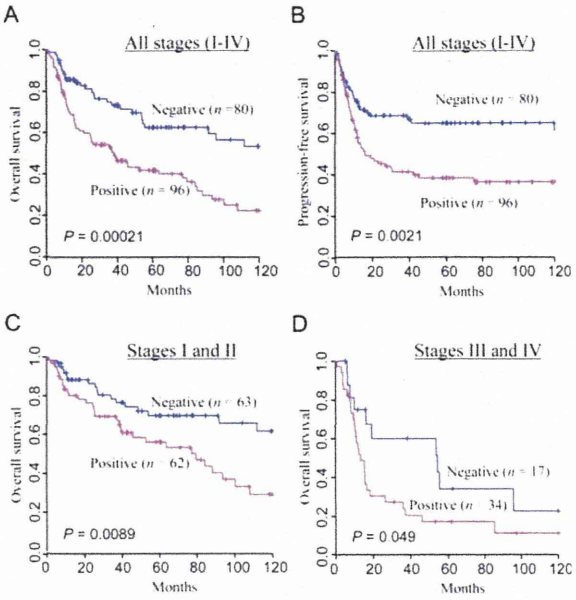

Figure 3. Survival of high-grade neuroendocrine tumour (HGNT) patients according to expression of the actinin-4 variant protein. Kaplan–Meier estimates of overall (A, C and D) and progression-free (B) survival for patients with all stages (A and B), stages I and II (C) and stages III and IV (D) HGNTs. Differences between the curves were assessed using the log-rank test.

patients whose tumours were positive were 42%, 32% and 49%, respectively. The prognostic significance of variant actinin-4 protein expression was reproducibly observed in subgroup analyses of patients with stages I and II and stages III and IV HGNT ($P = 0.0089$ and $P = 0.049$, respectively) (Figure 3C and D), whereas the expression of total actinin-4 proteins (detected by 13G9 monoclonal antibody) (supplementary Figure S4, available at *Annals of Oncology* online) or the three conventional NE markers (CGA, SYN and CD56) (supplementary Figure S5, available at *Annals of Oncology* online) did not show such prognostic significance.

Univariate analysis with the Cox proportional hazards model (Table 3) revealed that lymph node metastasis ($P = 0.000082$) and immunoreactivity for the actinin-4 splice variant ($P = 0.000467$) were significantly correlated with the outcome of the 173 patients with HGNTs. Multivariate analysis indicated that the expression of the actinin-4 splice variant was the most significant independent predictor of unfavourable outcome ($P = 0.00113$; hazard ratio (HR), 2.15; 95% confidence interval (CI) 1.36–3.40) after the presence of lymph node metastasis ($P = 0.00023$; HR, 2.25; 95% CI 1.46–3.47). The variant actinin-4 protein expression was also a significant independent predictor of outcome for SCLC (supplementary Table S2, available at *Annals of Oncology* online) ($P = 0.050$; HR, 2.16; 95% CI 1.00–4.68) and LCNEC (supplementary Table S3, available at *Annals of Oncology* online) ($P = 0.0038$; HR, 2.37; 95% CI 1.32–4.26).

discussion

In this study, we first determined the distribution of expression of the alternatively spliced *ACTN4* transcript in a large panel of human cancer cell lines derived from various tissues. We confirmed the frequent expression of *ACTN*-Va in SCLCs and the absence of its expression in NSCLCs. The variant transcript was also expressed frequently in choriocarcinoma, but its relationship with NE differentiation as well as its clinical significance remained undetermined. We then investigated the expression of the variant actinin-4 protein in a variety of histological subtypes of lung cancer using a newly established monoclonal antibody (Figure 1). We found that the expression pattern of the variant protein was apparently different from any of the conventional NE markers. CGA, SYN and CD56 were expressed in 76%–100% of pulmonary carcinoid tumours (Table 1), whereas the variant actinin-4 was expressed in only 10% (5/51) of them. The expression of variant actinin-4, but not that of CGA, SYN or CD56, was significantly associated with an unfavourable post-surgical outcome in HGNT patients (Figure 3 and supplementary Figure S5, available at *Annals of Oncology* online). These results indicated that variant actinin-4

Table 3. Hazard ratios for death in patients with high-grade neuroendocrine tumours

Variable		Univariate analysis			Multivariate analysis		
	N	HR	95% CI	*P* value	HR	95% CI	*P* value
Age							
<65/≥65 years	71/102	1.00	0.65–1.55	0.983			
Smoking history							
Absent/present	7/166	1.63	0.40–6.65	0.492			
Gender							
Female/male	33/140	1.12	0.64–1.96	0.683			
Tumour size							
≤3 cm/>3 cm	93/80	1.33	0.87–2.04	0.184			
Lymph node metastasis							
Absent/present	101/72	2.37	1.54–3.65	0.00008	2.25	1.46–3.47	0.00023
Distant metastasis							
Absent/present	167/6	1.70	0.69–4.20	0.249			
Adjuvant chemotherapy							
Yes/no	40/133	0.77	0.44–1.35	0.362			
Histological subtype							
LCNEC/SCLC	103/70	1.12	0.73–1.74	0.596			
Variant actinin-4 protein expression							
Negative/positive	79/94	2.27	1.43–3.59	0.000467	2.15	1.36–3.40	0.00113

Three patients with LCNEC, for whom no data regarding adjuvant therapy were available, were excluded from the analysis.
HR, hazard ratio; CI, confidence interval; LCNEC, large cell neuroendocrine carcinoma; SCLC, small cell lung carcinoma.

is not a simple marker for NE differentiation, but seems to be associated with the malignant progression of NE tumours.

We originally identified actinin-4 as an actin-bundling protein associated with enhanced cell motility and cancer invasion [9]. Actinin-4 directly regulates cell motility through remodelling of the actin cytoskeleton [9, 22]. Increased expression of actinin-4 protein is closely associated with a poor outcome in patients with breast cancer [9], colorectal cancer [22], pancreatic cancer [18], ovarian cancer [19] and NSCLC [23]. However, the expression of total actinin-4 protein (i.e. the ubiquitous and variant actinin-4 proteins together) detected by the monoclonal antibody 13G9 was not significantly correlated with the outcome of HGNT patients (supplementary Figure S4, available at *Annals of Oncology* online). The amino acid sequence encoded by exon 8 is crucial for the function of the *ACTN4* gene. In fact, a germline missense mutation in exon 8 is responsible for a hereditary renal disease, familial focal segmental glomerulosclerosis [24]. The splice variant as well as mutated actinin-4 proteins have a higher affinity for actin polymers [10]. SCLC shows an abnormal actin cytoskeleton structure [10]. Existing experimental data as well as the current clinical observations suggest that variant actinin-4 very likely plays a functional role in the aggressive behaviour of NE lung tumours. Because of its limited expression in normal tissues, variant actinin-4 may also serve as a therapeutic target.

If a biomarker capable of defining a subset of HGNT patients whose prognosis is likely to be unfavourable were to be identified, allowing them to be selected for intense adjuvant chemotherapy, then their survival might be improved. Recently Klotho was newly characterized as a biomarker predictive of a favourable outcome in patients with LCNEC [25] and limited-disease SCLC [26], although the number of cases examined was relatively small. The expression of CD117 was also reported to show marginally significant correlation with recurrence of LCNEC ($P = 0.046$) [27]. It is expected that combination of these emerging prognostic biomarkers with variant actinin-4 would further improve the accuracy of HNGT prognostication. Future investigation to select and validate an optimal biomarker set is anticipated.

funding

This study was supported by the Program for Promotion of Fundamental Studies in Health Sciences conducted by the National Institute of Biomedical Innovation of Japan, Research on Biological Markers for New Drug Development conducted by the Ministry of Health, Labor and Welfare of Japan and the National Cancer Center Research and Development Fund.

disclosure

The authors have declared no conflicts of interest.

references

1. Travis WD, Linnoila RI, Tsokos MG et al. Neuroendocrine tumors of the lung with proposed criteria for large-cell neuroendocrine carcinoma. An ultrastructural, immunohistochemical, and flow cytometric study of 35 cases. Am J Surg Pathol 1991; 15: 529–553.
2. Travis WD, Colby TV, Corrin B et al. World Health Organization International Histological Classification of Tumors. Histological Typing of Lung and Pleural Tumors, 3rd edition. Berlin: Springer 1999.
3. Cooper WA, Thourani VH, Gal AA et al. The surgical spectrum of pulmonary neuroendocrine neoplasms. Chest 2001; 119: 14–18.
4. Travis WD, Rush W, Flieder DB et al. Survival analysis of 200 pulmonary neuroendocrine tumors with clarification of criteria for atypical carcinoid and its separation from typical carcinoid. Am J Surg Pathol 1998; 22: 934–944.

5. Asamura H, Kameya T, Matsuno Y et al. Neuroendocrine neoplasms of the lung: a prognostic spectrum. J Clin Oncol 2006; 24: 70–76.
6. Travis WD. Advances in neuroendocrine lung tumors. Ann Oncol 2010; 21(Suppl 7): vii65–vii71.
7. Takei H, Asamura H, Maeshima A et al. Large cell neuroendocrine carcinoma of the lung: a clinicopathologic study of eighty-seven cases. J Thorac Cardiovasc Surg 2002; 124: 285–292.
8. Ionescu DN, Treaba D, Gilks CB et al. Nonsmall cell lung carcinoma with neuroendocrine differentiation—an entity of no clinical or prognostic significance. Am J Surg Pathol 2007; 31: 26–32.
9. Honda K, Yamada T, Endo R et al. Actinin-4, a novel actin-bundling protein associated with cell motility and cancer invasion. J Cell Biol 1998; 140: 1383–1393.
10. Honda K, Yamada T, Seike M et al. Alternative splice variant of actinin-4 in small cell lung cancer. Oncogene 2004; 23: 5257–5262.
11. Pio R, Montuenga LM. Alternative splicing in lung cancer. J Thorac Oncol 2009; 4: 674–678.
12. Sakaguchi N, Kimura T, Matsushita S et al. Generation of high-affinity antibody against T-cell-dependent antigen in the Ganp gene-transgenic mouse. J Immunol 2005; 174: 4485–4494.
13. Ono M, Matsubara J, Honda K et al. Prolyl 4-hydroxylation of alpha-fibrinogen: a novel protein modification revealed by plasma proteomics. J Biol Chem 2009; 284: 29041–29049.
14. Matsubara J, Ono M, Negishi A et al. Identification of a predictive biomarker for hematologic toxicities of gemcitabine. J Clin Oncol 2009; 27: 2261–2268.
15. Satow R, Shitashige M, Jigami T et al. β-Catenin inhibits promyelocytic leukemia protein tumor suppressor function in colorectal cancer cells. Gastroenterology 2012; 142: 572–581.
16. Travis WD, Brambilla E, Muller-Hermelink HK. World Health Organization Classification of Tumours. Pathology and Genetics of Tumours of the Lung, Pleura, Thymus and Heart. Lyon: IARC Press 2004.
17. Sobin L, Gospodarowicz M, Wittrkind C. TNM Classification of Malignant Tumors. New York: Wiley-Blackwell 2010.
18. Kikuchi S, Honda K, Tsuda H et al. Expression and gene amplification of actinin-4 in invasive ductal carcinoma of the pancreas. Clin Cancer Res 2008; 14: 5348–5356.
19. Yamamoto S, Tsuda H, Honda K et al. Actinin-4 expression in ovarian cancer: a novel prognostic indicator independent of clinical stage and histological type. Mod Pathol 2007; 20: 1278–1285.
20. Idogawa M, Yamada T, Honda K et al. Poly(ADP-ribose) polymerase-1 is a component of the oncogenic T-cell factor-4/beta-catenin complex. Gastroenterology 2005; 128: 1919–1936.
21. Yamaguchi U, Nakayama R, Honda K et al. Distinct gene expression-defined classes of gastrointestinal stromal tumor. J Clin Oncol 2008; 26: 4100–4108.
22. Honda K, Yamada T, Hayashida Y et al. Actinin-4 increases cell motility and promotes lymph node metastasis of colorectal cancer. Gastroenterology 2005; 128: 51–62.
23. Yamagata N, Shyr Y, Yanagisawa K et al. A training-testing approach to the molecular classification of resected non-small cell lung cancer. Clin Cancer Res 2003; 9: 4695–4704.
24. Kaplan JM, Kim SH, North KN et al. Mutations in ACTN4, encoding alpha-actinin-4, cause familial focal segmental glomerulosclerosis. Nat Genet 2000; 24: 251–256.
25. Usuda J, Ichinose S, Ishizumi T et al. Klotho is a novel biomarker for good survival in resected large cell neuroendocrine carcinoma of the lung. Lung Cancer 2011; 72: 355–359.
26. Usuda J, Ichinose S, Ishizumi T et al. Klotho predicts good clinical outcome in patients with limited-disease small cell lung cancer who received surgery. Lung Cancer 2011; 74: 332–337.
27. Casali C, Stefani A, Rossi G et al. The prognostic role of c-kit protein expression in resected large cell neuroendocrine carcinoma of the lung. Ann Thorac Surg 2004; 77: 247–252.

British Journal of Cancer (2012) 106, 867–875

www.bjcancer.com

Enzastaurin has anti-tumour effects in lung cancers with overexpressed JAK pathway molecules

T Shimokawa[1], M Seike*[,1], C Soeno[1], H Uesaka[2], A Miyanaga[1], H Mizutani[1], K Kitamura[1], Y Minegishi[1], R Noro[1], T Okano[1], A Yoshimura[1] and A Gemma[1]

[1]Department of Internal Medicine, Division of Pulmonary Medicine/Infection and Oncology, Nippon Medical School, 1-1-5, Sendagi, Bunkyo-ku, Tokyo 113-8603, Japan; [2]MediBIC, Tokyo, Japan

BACKGROUND: Enzastaurin, an oral serine–threonine kinase inhibitor, was initially developed as an ATP-competitive selective inhibitor against protein kinase Cβ. However, the mechanism by which enzastaurin contributes to tumourigenesis remains unclear.

METHODS: We analysed the anti-tumour effects of enzastaurin in 22 lung cancer cell lines to ascertain the potential for enzastaurin-based treatment of lung cancer. To identify molecules or signalling pathways associated with this sensitivity, we conducted a gene, receptor tyrosine kinases phosphorylation and microRNA expression profiling study on the same set of cell lines.

RESULTS: We identified eight genes by pathway analysis of molecules having gene-drug sensitivity correlation, and used them to build a support vector machine algorithm model by which sensitive cell lines were distinguished from resistant cell lines. Pathway analysis revealed that the JAK/STAT signalling pathway was one of the main ones involved in sensitivity to enzastaurin. Overexpression of JAK1 was observed in the sensitive cells by western blotting. Simultaneous administration of enzastaurin and JAK inhibitor inhibited enzastaurin-induced cell growth-inhibitory effect. Furthermore, lentiviral-mediated JAK1-overexpressing cells were more sensitive to enzastaurin than control cells.

CONCLUSION: Our results suggested that the JAK1 pathway may be used as a single predictive biomarker for enzastaurin treatment. The anti-tumour effect of enzastaurin should be evaluated in lung cancer with overexpressed JAK pathway molecules.

British Journal of Cancer (2012) **106,** 867–875. doi:10.1038/bjc.2012.7 www.bjcancer.com
Published online 14 February 2012

Keywords: lung cancer; enzautaurin; PKC inhibitor; gene expression; drug sensitivity

Translational Therapeutics

Non-small-cell lung cancer (NSCLC) patients are usually diagnosed with advanced disease, and their prognosis remains poor despite improvements in chemotherapies (Mountain, 1997; Schiller *et al*, 2002; Ohe *et al*, 2007; Jemal *et al*, 2009). Recently, molecular-targeted therapies have been developed for NSCLC treatment. For example, NSCLC patients with epidermal growth factor receptor (EGFR) mutations have shown a dramatic response to EGFR inhibitors such as gefitinib and erlotinib (Mok *et al*, 2009; Maemondo *et al*, 2010). However, there remain many other molecular abnormalities in lung cancer that are as yet unexplored (Salgia and Skarin, 1998).

The protein kinase C (PKC) family of serine–threonine protein kinases has been implicated in several important cellular functions including proliferation, motility, invasion and apoptosis (Livneh and Fishman, 1997). Among the PKC isoforms, PKCβ is known to be an important mediator of vascular endothelial growth factor (VEGF) (Xia *et al*, 1996; Yoshiji *et al*, 1999), the most potent angiogenic factor found in various tumours. Increased invasion and proliferation in tumours have also been associated with PKCβ (Zhang *et al*, 2004). Overexpression and increased activity of PKCβ have been implicated in transformation and tumourigenesis in lung cancer (Barr *et al*, 1997; Lahn *et al*, 2006). In several human cancers, PKCβ expression is linked to poor prognosis, most notably in B-cell lymphoma (Shipp *et al*, 2002; Li *et al*, 2007). Biochemical analysis demonstrated that PKCβ could target the phoshatidylinositol 3-kinase (PI3K)/AKT pathway and other signal transduction pathways (Graff *et al*, 2005; Rascoe *et al*, 2005). However, the mechanism by which PKCβ contributes to tumourigenesis remains unclear.

The PKCβ inhibitor enzastaurin, an oral serine–threonine kinase inhibitor, was initially developed as an ATP-competitive selective inhibitor against PKCβ (Faul *et al*, 2003). Enzastaurin is now being evaluated in several phase II studies across a variety of more common tumour types including: breast, ovarian colon and prostate cancers (Mina *et al*, 2009; Vergote *et al*, 2009; Dreicer *et al*, 2010; Glimelius *et al*, 2010). It has also been evaluated as second- or third-line therapy for NSCLC in a phase II study (Oh *et al*, 2008; Chiappori *et al*, 2010). *In vitro*, sequence-dependent, synergistic anti-proliferative and proapoptotic effects of the combination of cytotoxic drugs and enzastaurin have been found in NSCLC cells (Rademaker-Lakhai *et al*, 2007; Morgillo *et al*, 2008; Tekle *et al*, 2008). These studies suggest that enzastaurin may have an activity against lung cancer.

In this study, we analysed the anti-tumour effects of enzastaurin in a panel of 22 lung cancer cell lines to ascertain the potential for enzastaurin-based treatment of lung cancer. We also conducted gene, receptor tyrosine kinases (RTKs) phosphorylation and microRNA (miRNA) profiling on the same set of cell lines to identify the molecules associated with sensitivity of lung cancer to enzastaurin treatment. The correlation between the cytotoxic activity of enzastaurin and the corresponding gene, RTKs phosphorylation and miRNA expression patterns has been examined to clarify the

*Correspondence: Dr M Seike; E-mail: mseike@nms.ac.jp
Revised 8 December 2011; accepted 5 January 2012; published online 14 February 2012

responsible mechanisms of the signalling pathway involved in the response of lung cancers to enzastaurin treatment.

MATERIALS AND METHODS

Cell lines

We used 22 lung cancer cell lines: A549, PC3, PC7, PC9, PC14, LC2/ad, ABC-1, RERF-LC-KJ, RERF-LC-MS, RERF-LC-AI adenocarcinoma (AC) cell lines and PC1, PC10, LK2, SQ5, QG56, EBC-1, LC1/sq squamous-cell carcinoma (SCC) cell lines and NCI-H69, NCI-N231, Lu135, SBC3, MS-1 small-cell lung carcinoma (SCLC) cell lines for this study. In addition, five cell lines comprising H1650, H1975, LC-1F, RERF-LC-OK and VMRC-LCD, were used as the test set for a validation study. A549, NCI-H69, NCI-N231, H1650 and H1975 were purchased from the American Type Culture Collection (ATCC, Manassas, VA, USA); RERF-LC-KJ, RERF-LC-AI, RERF-LC-OK, LC2-ad, SQ5, LC2/Ad, LC1/Sq, LC-1F and MS-1 were obtained from the RIKEN Cell Bank (Ibaraki, Japan) and PC1, PC3, PC7, PC9, PC10 and PC14 were obtained from Immuno-Biological Laboratories (Gunma, Japan); RERF-LC-MS, ABC-1, EBC-1, LK2, QG56 and VMRC-LCD were purchased from Health Science Research Resources Bank (Osaka, Japan). Lung cancer cell lines were maintained in RPMI 1640 medium (GIBCO, Carlsbad, CA, USA) supplemented with 10% fetal bovine serum.

Drugs and growth-inhibition assay

Enzastaurin was kindly provided by Ely Lilly. Growth inhibition was assessed by MTS assay to examine the effect of enzastaurin on lung cancer cell lines. Cell suspensions (5000 cells per well) were seeded into 96-well plates and increasing concentrations of enzastaurin (0, 0.01, 0.1, 1.0, 10 and 100 μM) were added. After incubation for 72 h at 37 °C, MTS was added to each well and incubated for 2 h at 37 °C, after which absorbance was measured using a microplate reader with a test wavelength of 450 nm. The IC_{50} value was defined as the concentration needed for 50% reduction of the growth by treatment with enzastaurin.

JAK inhibitor (JAK inhibitor I, Cat. No 420099) was purchased from Calbiochem (San Diego, CA, USA). A549 and RERF-LC-KJ cells (5000 cells per well) were seeded into 96-well plates. After 24 h, the cells were incubated for 72 h in the various concentrations of enzastaurin (0, 0.01. 0.1, 1.0, 10 and 100 μM), with or without low-dose (1 μM) JAK inhibitor.

RNA isolation, cDNA array, RTKs phosphorylation antibody array and miRNA array

Total RNA was isolated from lung cancer cell lines with the use of TRIzol reagent (Invitrogen, Carlsbad, CA, USA), according to the manufacturer's instructions. High-density oligonucleotide array analysis was carried out using Affymetrix HG-U133A (22 282 probe sets) expression array, as previously described (Gemma *et al*, 2006). Scanning was performed with the GeneChip Scanner 3000 (Affymetrix, Santa Clara, CA, USA), and GeneChip analysis was based on the Affymetrix GeneChip Manual with GeneChip Operating Software version 1.0 (Affymetrix), and Microarray Database software. We also performed human RTKs phosphorylation antibody array, including 71 antibodies (RayBiotech, Inc., Norcross, GA, USA). MicroRNA expression profiles were analysed by TaqMan MicroRNA Array set version 2.0 containing 667 miRNAs and validated by TaqMan MicroRNA assay (Applied Biosystems, Foster City, CA, USA).

Western blot analysis

Cells were lysed in buffer containing 50 mM Tris–HCl, pH 7.6, 150 mM NaCl, 0.1% sodium dodecyl sulphate, 1% Nonidet P-40 and 0.5% sodium deoxycholate. The lysates were kept on ice for 30 min, and then centrifuged at 13 000 g for 30 min. The supernatant was collected and 10 μg of protein were separated by gel electrophoresis on 10% gels, transferred to nitrocellulose membranes and detected by immunoblotting using a chemiluminescence system (GE Healthcare Bio-Sciences Corp., Piscataway, NJ, USA). The antibodies detecting JAK1, STAT3, phospho-STAT3 (p-STAT) and β-actin were purchased from Cell Signaling Technology (Beverley, MA, USA).

Lentiviral-mediated JAK1-overexpressing cells

Expression plasmid vector pEZ-Lv151 was used for lentiviral vector production (GeneCopoeia, Rockville, MD, USA). The coding sequence of human JAK1 or enhanced green fluorescent protein (EGFP) was inserted under the transcriptional control of the CMV promoter in pEZ-Lv151. The human JAK1 lentiviral expression plasmid (Ex-T8644-Lv151) or EGFP plasmid (Ex-EGFP-Lv151) was cotransfected into 293Ta cells with the Lenti-Pac HIV Packaging Mix (GeneCopoeia). Lentivirus-containing supernatants were harvested 48 h after transfection. The lentivirus particles were purified and stored at −80 °C in aliquots until use.

To establish stable JAK1-overexpressing cell lines, A549 cells were transduced with serial dilutions of lentiviral supernatant in the presence of 5 $\mu g\,ml^{-1}$ polybrene and selected by 0.8 $ng\,ml^{-1}$ geniticine. After antibiotic selection for 3 weeks, stable overexpressing JAK1 cells (LV-JAK1 A549 cells) were obtained.

Statistical analyses

Data analysis for the correlation coefficients that revealed the correlation between the drug activity patterns and the gene expression patterns was principally done by a modified National Cancer Institute programme (Miyanaga *et al*, 2008). We used pathway analysis to provide a viewpoint of the biological function of genes within the proposed classifier. Pathway analysis was done using the Pathway Architect software (Stratagene, La Jolla, CA, USA). The pathways showing the relationships among the genes on the list were drawn by selecting all molecules on the pathway edit window. All relationships among the molecules were retrieved from the database, with this information being derived from PubMed abstracts by natural language processing technology. The function was done by selecting the data of maximum reliability (MAX) by choosing all modes of interactions including 'Promoter Binding', 'Regulation', 'Protein Modification' and 'Expression' and by taking the relationships supported by three or more consistent data sources. Next, we picked out the incorporated genes from the imported gene list used at the onset of the pathway analysis, except the subunits of the target gene. Thus, a list of the genes associated with drug response was established with respect to not only gene expression profile data but also the biological functions of altered/associated genes. Data from the listed genes were used to build a support vector machine (SVM) model with ArrayAssist software (Stratagene) to predict the drug response (IC_{50}). The SVM algorithm model with Gaussian kernels was used to distinguish sensitive cells from resistant cells, using biomarkers identified by the gene expression-enzastaurin drug sensitivity correlation and pathway analysis. The classification ability of the genes was evaluated using leave-one-out cross-validation.

RESULTS

Effect of enzastaurin on the growth of lung cancer cells

Growth-inhibitory effects of enzastaurin on lung cancer cell lines were assessed by MTS assay.

Figure 1 shows the sensitivity to enzastaurin among the 22 lung cancer cells. Based on the IC_{50}, the 22 cell lines were classified into two groups, namely: enzastaurin sensitive and enzastaurin

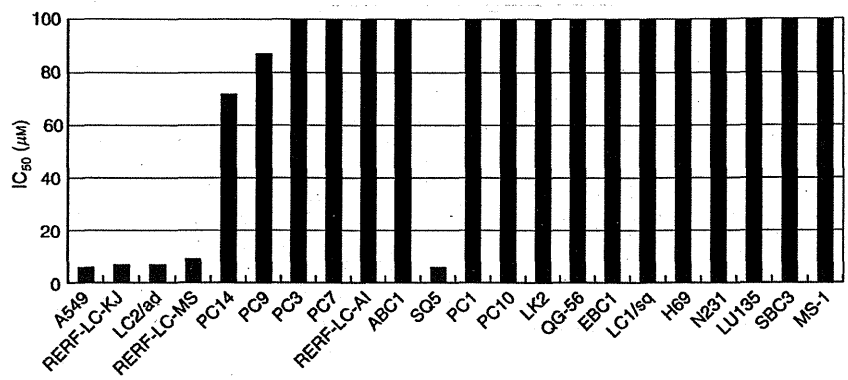

Figure 1 IC_{50} values for 22 lung cancer cell lines responding to enzastaurin treatment by MTS assay. According to sensitivity to enzastaurin, these 22 cell lines were classified as sensitive (IC_{50} of $\leqslant 10\,\mu M$) or resistant (IC_{50} of $>50\,\mu M$).

Table 1 Unique genes correlated with sensitivity to enzastaurin

Gene symbol	Gene title	F-statistic	*P*-value	Correlation coefficients	Eight-gene predictor
DUSP1	Dual specificity phosphatase 1	49.2	8.39E−07	−0.69	*
ILF3	Interleukin enhancer binding factor 3, 90 kDa	48.5	1.10E−06	0.67	*
LITAF	Lipopolysaccharide-induced TNF factor	36.0	9.75E−06	−0.70	*
JAK1	Janus kinase 1 (a protein tyrosine kinase)	27.1	6.36E−05	−0.65	*
COPS7B	COP9 constitutive photomorphogenic homologue subunit 7B (Arabidopsis)	19.3	5.48E−04	0.66	*
RAD23A	RAD23 homologue A (*S. cerevisiae*)	23.0	9.10E−04	0.74	*
TNFAIP1	Tumour necrosis factor, α-induced protein 1 (endothelial)	19.5	0.002	−0.65	*
MIRN21///TMEM49	Transmembrane protein 49///microRNA 21	14.1	0.003	−0.66	*
PSEN1	Presenilin 1 (Alzheimer disease 3)	9.5	0.012	−0.65	
PPAP2A	Phosphatidic acid phosphatase type 2A	11.3	0.014	−0.75	
IGF1R	Insulin-like growth factor 1 receptor	10.6	0.019	−0.66	
SART3	Squamous cell carcinoma antigen recognised by T cells 3	9.4	0.019	0.65	
NDFIP1	Nedd4 family interacting protein 1	6.0	0.029	−0.66	
MLPH	Melanophilin	8.2	0.034	−0.65	
SEMA3C	Sema domain, immunoglobulin domain (Ig), short basic domain, secreted (semaphorin) 3C	5.9	0.056	−0.67	
UGDH	UDP-glucose dehydrogenase	5.9	0.062	−0.68	

Abbreviations: ANOVA = analysis of variance; TNF = tumour necrosis factor. Note: F-statistic and *P*-values were calculated by ANOVA. *Genes used as eight-gene predictor are shown.

resistant. Five cell lines (A549, RERF-LC-KJ, LC2/ad, RERF-LC-MS and SQ5) were sensitive (IC_{50} of $\leqslant 10\,\mu M$), and the remaining 17 cell lines were resistant to enzastaurin (IC_{50} of $>50\,\mu M$). The five cell lines sensitive to enzastaurin consisted of four AC (4/10, 40%) and one SCC (1/7, 14%) cell line; no SCLC (0/5) cell lines were enzastaurin sensitive. These results suggest that enzastaurin has anti-tumour activity against NSCLC.

Gene expression-drug sensitivity correlation

We have previously performed gene expression profile analysis of the same set of 22 lung cell lines by Affymetrix GeneChip (Gemma *et al*, 2006). First, we used the MTS results for enzastaurin for the development of a molecular model of sensitivity to enzastaurin. Twenty-three genes were significantly correlated with sensitivity to enzastaurin (correlation coefficients of >0.65). Next, pathway analysis was performed using the 23 genes to provide a viewpoint of the biological function of the genes, as previously described (Miyanaga *et al*, 2008). Pathway analysis removed the incorporated genes out of the imported 23 genes. Sixteen genes, associated with sensitivity to enzastaurin, were identified based on the biological functions of altered/associated genes (Table 1; Figure 2A). Pathway analysis revealed that JAK1 was the final target gene for the sensitivity to enzastaurin in lung cancer cells (Figure 2A). We next identified the optimal number of genes whose expression could accurately distinguish the sensitive cells from the resistant ones. Analysis of variance (ANOVA) was done to remove the genes with variance. The top eight genes (DUSP1, ILF3, LITAF, JAK1, COPS7B, RAD23A, TNFAIP1 and MIRN21/TMEM49) according to the ANOVA were subsequently found to be the minimum number necessary for prediction of drug response (Figure 2B; Table 1). We used the eight most strongly correlated genes to build an SVM algorithm model by which the five sensitive cells were distinguished from the 17 resistant cells. Overall, the SVM classification based on the above-mentioned eight genes, correctly classified the sensitivity to enzastaurin of all of the 22 cells (data not shown). Next, we examined the robustness of the eight-gene predictor, for classifying cells into the enzastaurin-sensitive group, in an independent set of NSCLC cells, and found that the eight-gene predictor correctly classified all five resistant cells (Table 2). Thus, we had ultimately identified an eight-gene signature that was validated for its ability to predict the sensitivity to enzastaurin in an independent set of lung cancer cells.

RTKs phosphorylation and miRNA expression-drug sensitivity correlation

Pathway analysis revealed that JAK1 was an important gene for the sensitivity to enzastaurin in lung cancer cells. JAK1 and its downstream STAT3 gene expression levels of sensitive cells were

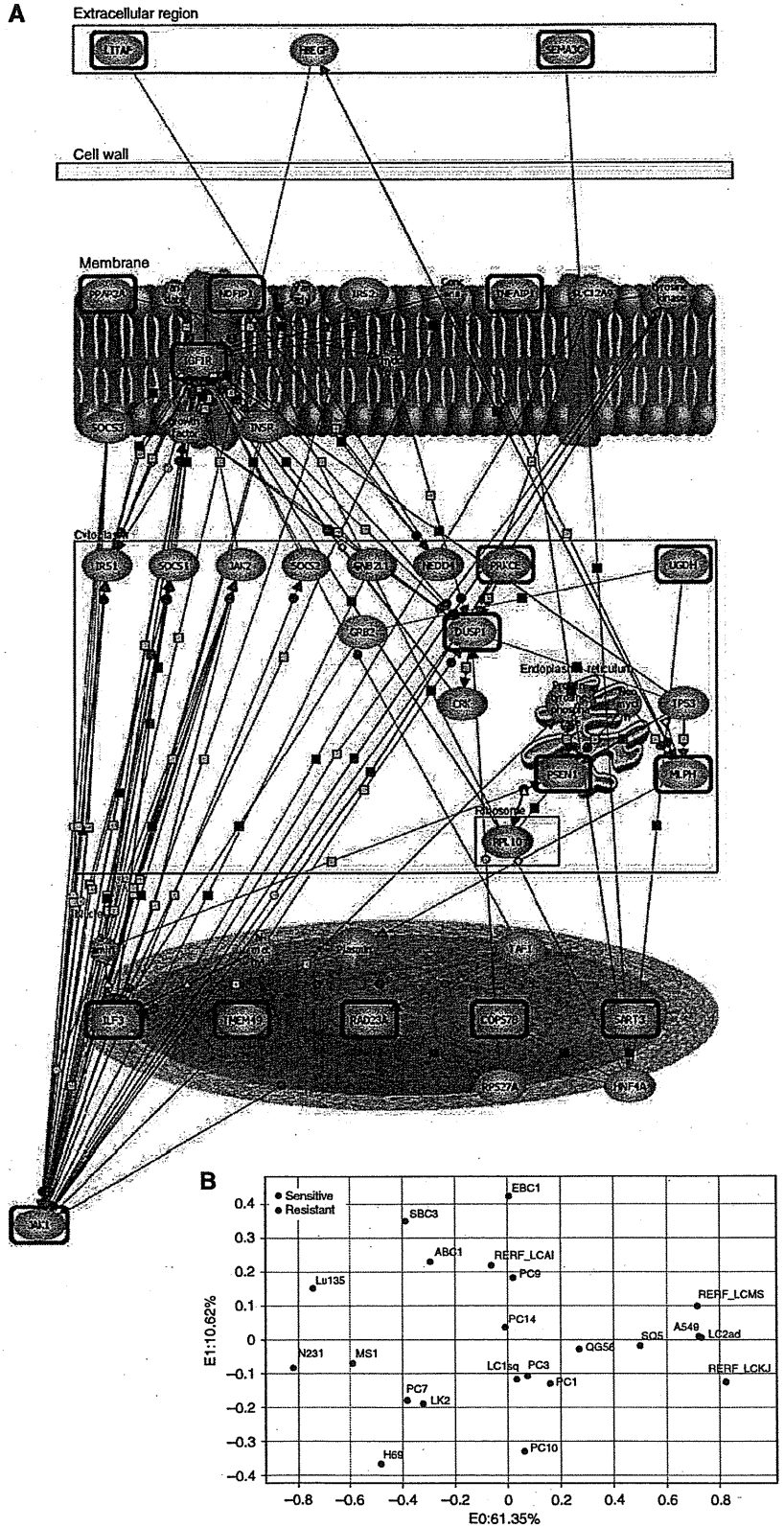

Figure 2 Sixteen genes associated with enzastaurin response were established by pathway analyses and prediction of drug response using an eight-gene signature. (**A**) Sixteen genes (blue circle) associated with enzastaurin response and PKC (red circle) belonged to the same signal pathway. (**B**) Principal component analysis based on the eight-gene profile correctly distinguished the sensitive cells from the resistant ones. The colour reproduction of this figure is available at the *British Journal of Cancer* online.

significantly higher than those of resistant cells (Figures 3A and B). To further clarify the signalling mechanism correlated with the sensitivity to enzastaurin, we also examined RTKs phosphorylation expression profiles of the same set of 22 lung cancer cells. The top 10 RTKs phosphorylation associated with enzastaurin sensitivity are shown in Table 3 (correlation coefficients of >0.50). Pathway analysis using the 23 genes and 10 RTKs phosphorylation associated with sensitivity to enzastaurin also revealed that JAK/STAT signal pathway was mainly involved in the drug response (data not shown). Among the 10 RTKs phosphorylation, the expression of two RTKs mainly associated with angiogenesis and lymphangiogenesis (VEGFR2 and VEGFR3) was significantly elevated in sensitive cells compared with in resistant cells (Figures 3C and D).

Table 2 Validation of the eight-gene predictor by examining the SVM value in an independent set of five NSCLC cell lines

		Histology	IC_{50} (μM)	Predicted class*
1	H1650	AC	>100	Resistant
2	H1975	AC	>100	Resistant
3	RERF-LC-OK	AC	>100	Resistant
4	VMRC-LCD	AC	>100	Resistant
5	LC-1F	SCC	>100	Resistant

Abbreviations: AC = adenocarcinoma; SVM = support vector machine; NSCLC = non-small-cell lung cancer. Note: *Cell lines were classified as sensitive (IC_{50} of $\leq 10\,\mu$M) and resistant (IC_{50} of $>50\,\mu$M) to enzastaurin.

Table 3 Kinase and miRNA correlated with the sensitivity to enzastaurin

	Kinase	F-statistic	P-value	Correlation coefficients
(a)				
1	M-CSFR	11.51	0.02	−0.82
2	VEGFR2	9.17	0.03	−0.68
3	FER	9.00	0.02	−0.60
4	EphA1	7.58	0.02	−0.61
5	VEGFR3	6.76	0.05	−0.58
6	TNK1	4.45	0.09	−0.71
7	NGFR	3.73	0.11	−0.68
8	MATK	2.95	0.15	−0.52
9	Hck	2.26	0.20	−0.53
10	SYK	1.82	0.23	−0.58
	miRNA	**F-statistic**	**P-value**	**Correlation coefficients**
(b)				
1	hsa-miR-15a*	18.56	0.0004	0.51
2	hsa-miR-454*	16.65	0.0006	0.53
3	hsa-miR-92a	15.96	0.0007	0.52
4	hsa-miR-301b	12.49	0.0021	0.54
5	hsa-miR-130b	11.85	0.0026	0.54
6	hsa-miR-106b*	11.42	0.0032	0.52
7	hsa-miR-345	9.25	0.01	0.54
8	hsa-miR-31	7.25	0.05	−0.76
9	hsa-let-7a	4.04	0.09	0.54
10	hsa-miR-193b	2.76	0.14	−0.64
11	hsa-miR-193b*	2.76	0.15	−0.61
12	hsa-miR-21	2.24	0.18	−0.53
13	hsa-miR-30c-2*	1.93	0.24	−0.52

Abbreviations: ANOVA = analysis of variance; miRNA = microRNA. Note: F-statistic and P-values were calculated by ANOVA. *The miRNA name used in TaqMan microRNA array analysis.

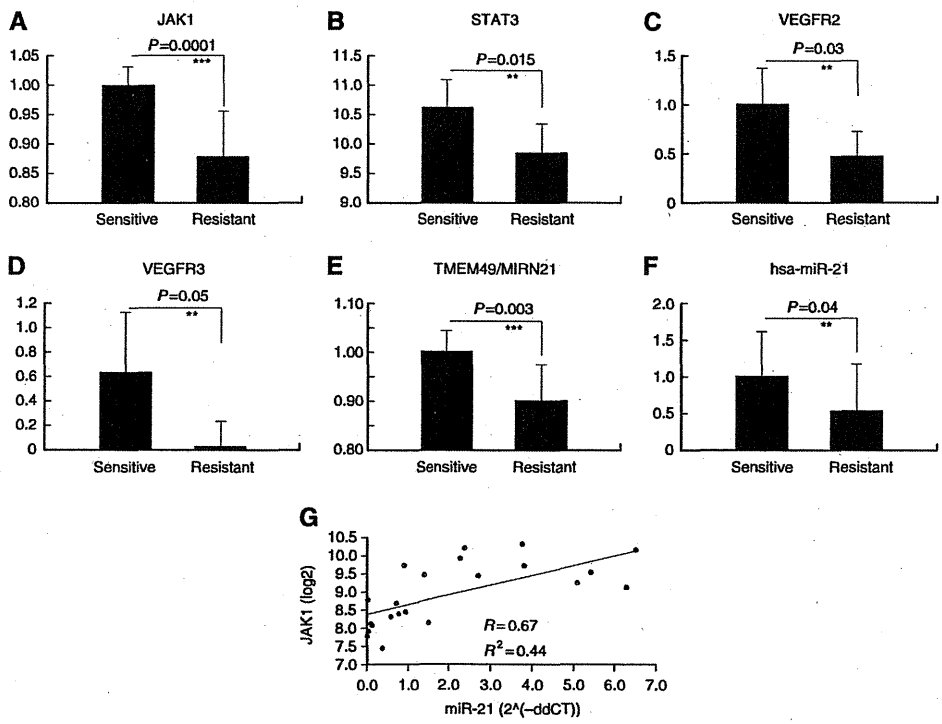

Figure 3 JAK1, VEGFR2, VEGFR3 and miR-21 were correlated with drug response. (**A** and **B**) JAK1 and STAT3 gene expression levels were significantly higher in the sensitive cell group than in the resistant cell group. (**C** and **D**) Elevated levels of VEGFR2 and VEGFR3 expression were observed in sensitive cells. (**E**) Expression of MIRN21/TMEM49 was significantly higher in sensitive cells than in resistant cells, by gene-chip analysis. (**F**) Mature miR-21 expression was significantly higher in sensitive cells than in resistant cells by quantitative RT–PCR analysis. (**G**) Quantitative comparison of miR-21 and JAK1 showed a significant positive correlation between these two molecules. **$P<0.05$ when compared with the resistant cells. ***$P<0.01$ when compared with the resistant cells.

In order to investigate post-transcriptional regulation, miRNA microarray analysis of the 22 cells was also performed. We identified 13 miRNAs correlated with enzastaurin sensitivity (correlation coefficients of >0.50) (Table 3). Interestingly, MIRN21/TMEM49, a host gene of miR-21, was included among the eight genes associated with enzastaurin sensitivity, and was expressed at significantly higher levels in sensitive cells compared with in resistant cells (Figure 3E). In addition, a correlation between miR-21 and enzastaurin sensitivity was found in miRNA array analysis (correlation coefficients -0.53) (Table 3). Recent reports demonstrated that miR-21 is a major miRNA that may play an oncogenic role in lung carcinogenesis (Volinia *et al*, 2006; Yanaihara *et al*, 2006; Seike *et al*, 2009). The expression levels of miR-21 were examined by real-time quantitative RT–PCR. miR-21 expression was significantly higher in sensitive cells than in resistant cells ($P<0.05$, paired *t*-test) (Figure 3F). The quantitative comparison of miR-21 and JAK1 showed a significant positive correlation between these two (Pearson's correlation, $r=0.67$, $P<0.05$) (Figure 3G). We ultimately recognised JAK1, VEGFR2, VEGFR3 and miR-21 as factors concerned with sensitivity to enzastaurin. In particular, JAK1 is the most significant molecule involved in drug response.

JAK1 expression effect on drug sensitivity in A549 cells

To investigate further the effect of JAK1 on sensitivity to enzastaurin, JAK1 protein expression of 11 NSCLC cells was evaluated by western blot analysis. Elevated JAK1 protein was observed in enzastaurin-sensitive NSCLC cells (Figure 4A). Next, we inhibited JAK1 protein using JAK1 inhibitor in enzastaurin-sensitive A549 and RERF-LC-KJ cells. After the treatment of JAK inhibitor (1 μM), JAK1 and its downstream p-STAT3 expression was completely diminished until 72 h in A549 cells (Figure 4B). We examined the effect of enzastaurin and JAK inhibitor combination therapy on cell growth. Concurrent JAK inhibitor and enzastaurin therapy significantly decreased the growth-inhibitory effect of enzastaurin, compared with enzastaurin monotherapy in enzastaurin-sensitive A549 cells (Figure 4C). Enzastaurin therapy after JAK inhibitor 1 μM treatment also diminished the growth-inhibitory effect of enzastaurin, compared with enzastaurin monotherapy in A549 cells (Figure 4D). The IC_{50} values of concurrent enzastaurin with JAK inhibitor and enzastaurin therapy after JAK inhibitor were 76 and 83, respectively, whereas that of enzastaurin monotherapy was 5.8 (Figures 4C and D). In addition, RERF-LC-KJ cells, which are also sensitive to

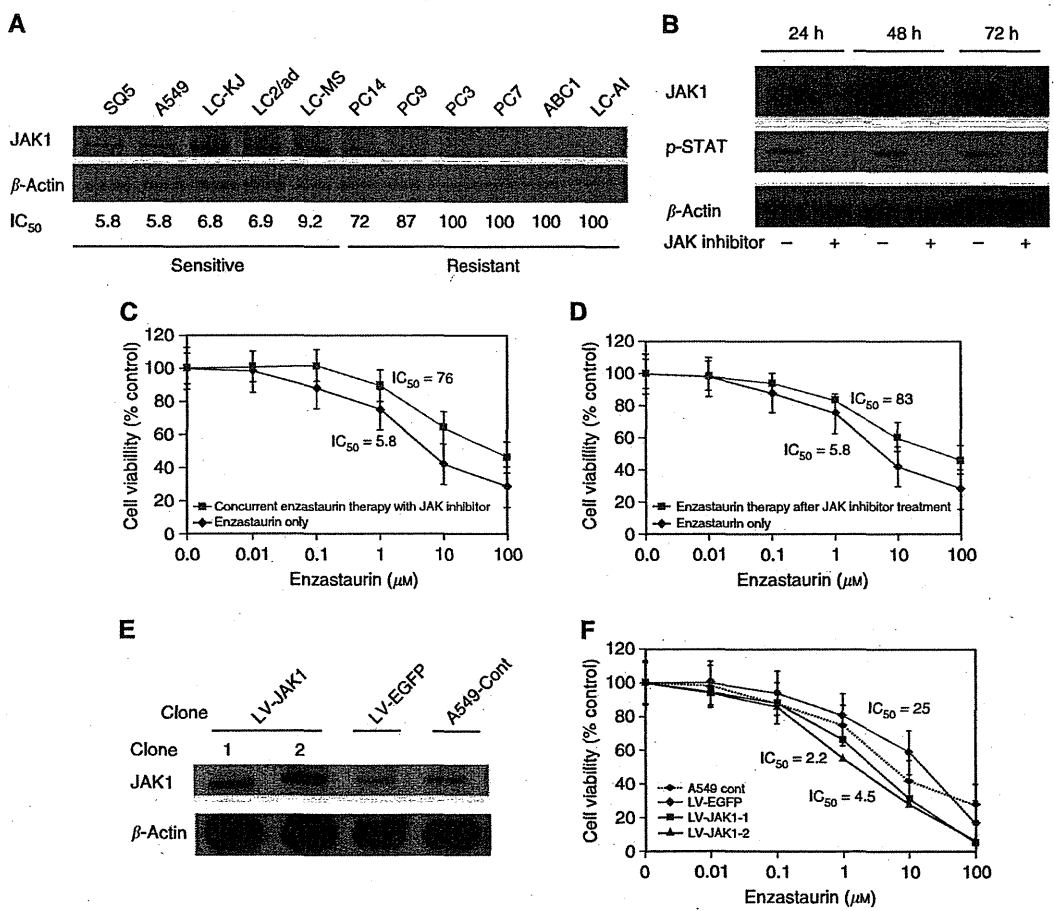

Figure 4 Effect of combination therapy with enzastaurin and JAK1 expression on cell growth in lung cancer cells. (**A**) JAK1 expression levels were significantly higher in the sensitive cell group than in the resistant cell group, by western blotting. (**B**) Completed inhibition of JAK1/STAT signalling by JAK1 inhibitor in A549 cells. P-STAT3 was completely inhibited until 72 h after the treatment of 1 μM JAK inhibitor. (**C**) Enzastaurin treatment with JAK inhibitor for 72 h was examined in A549 cells. Each result is expressed as cell viability in treated samples compared with the untreated sample (100%) for enzastaurin alone and concurrent therapy with the 1 μM JAK inhibitor treatment. (**D**) The effect of JAK inhibitor treatment (1 μM) for 24 h followed by enzastaurin treatment for 72 h was examined in A549 cells. (**E**) Lentiviral-mediated production of JAK1 in A549 cells. Western blotting showed that JAK1 expression levels were significantly higher in two LV-JAK1 clones than in the control clones. (**F**) Enzastaurin treatment for 72 h was examined in LV-JAK1-A549 cells. Each result is expressed as cell viability in the treated samples compared with the untreated sample (100%) for enzastaurin therapy.

enzastaurin, showed resistance after JAK inhibitor therapy in combination with enzastaurin (data not shown). In RERF-LC-KJ cells, both IC_{50} values of concurrent enzastaurin with JAK inhibitor and enzastaurin therapy after JAK inhibitor were over 100, whereas that of enzastaurin monotherapy was 6.8. To confirm further the ability of JAK1 to indicate drug sensitivity to enzastaurin, we developed a lentiviral vector for the expression of JAK1 and established stable JAK1-overexpressing A549 cells (LV-JAK1-A549 cells). Western blot analysis showed the overexpression of JAK1 in LV-JAK1-A549 cells (Figure 4E). The growth-inhibitory effect of enzastaurin on LV-JAK1-A549 cells was assessed by MTS assay. The drug sensitivities of two LV-JAK1-A549 cells were greater than those in the control cells (Figure 4F). The IC_{50} values of two LV-EGFP A549 cells were 2.2 and 4.5, respectively, whereas that of LV-EGFP A549 cells was 25 (Figure 4F). These results indicate that JAK1 expression contributed to the drug sensitivity and could be used as a drug-sensitive marker to enzastaurin in lung cancer cells.

JAK/STAT3 pathway directly activates miR-21

A significant correlation between JAK1 and miR-21 was found in our set of NSCLC cells (Figure 3G). STAT3 is a transcription factor activated by JAK1, and its binding to the target sites in miR-21 promoter upon IL-6 induction has been reported previously (Löffler *et al*, 2007; Iliopoulos *et al*, 2010). To verify the association between JAK1 and miR-21, miR-21 expression was quantified after the stimulation of IL-6 by qRT–PCR analysis. Upon IL-6 exposure, p-STAT3 expression was significantly upregulated, resulting in the overexpression of miR-21 at 24 h in A549 cells (Figures 5A and B). We also evaluated the miR-21 expression in LV-LAK1 A549 cells. In the JAK1-overexpressing cells, miR-21 expression was significantly higher than in parent cells (Figure 5C). These results supported the concept that miR-21 is directly induced by JAK/STAT signalling in NSCLC cells.

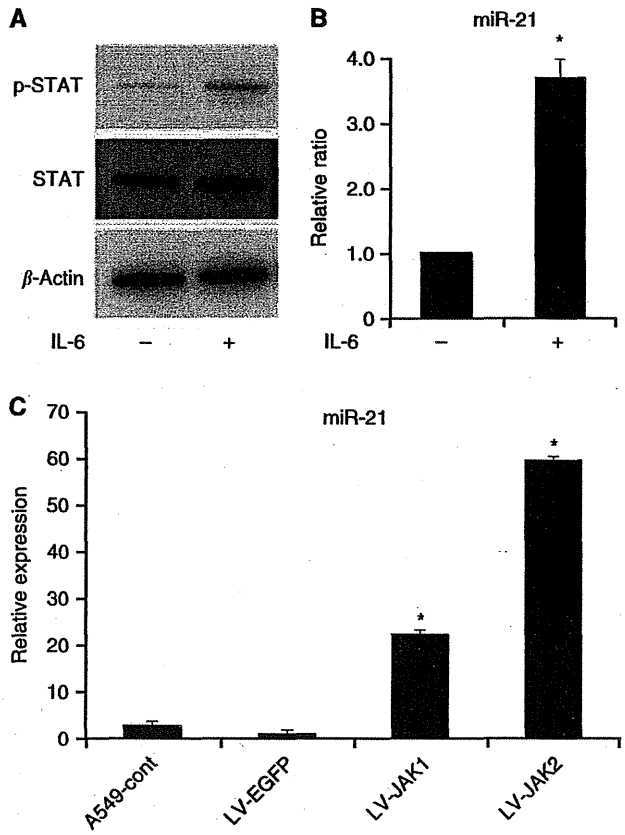

Figure 5 Association between JAK1 and miR-21 expression. (**A**) p-STAT3 was overexpressed after IL-6 stimulation of A549 cells for 24 h. (**B**) After IL-6 stimulation, miR-21 expression was significantly increased, as measured by qRT–PCR analysis. (**C**) MiR-21 expression of two LV-JAK1 cells was significantly higher than in the control cells, as measured by qRT–PCR analysis. Data were mean ± s.d. from three independent experiments. *$P<0.05$ when compared with the respective parent cells.

DISCUSSION

Enzastaurin has recently been evaluated as second- or third-line therapy of NSCLC in a phase II study (Oh *et al*, 2008; Chiappori *et al*, 2010). Synergistic effects of the combination of enzastaurin and cytotoxic drugs including cisplatin, gemcitabine and pemetrexed have been found in NSCLC cells in an *in vitro* study (Rademaker-Lakhai *et al*, 2007; Morgillo *et al*, 2008; Tekle *et al*, 2008). A recent study showed that enzastaurin inhibited *in vivo* metastasis of NSCLC cells (Körner *et al*, 2010). It is known that PKCs mediate the regulation of the cell cycle; enzastaurin is also able to inhibit several proteins involved in cell-cycle regulation, for example, E2F-1 associated with G1/S checkpoint and Cdc25C resulting in G2/M checkpoint (Tekle *et al*, 2008). These checkpoint arrests provide the tumour cells with the opportunity to repair their DNA, which has been damaged by cytotoxic drugs. Reduction of E2F-1 expression and phosphorylated Cdc25C by enzastaurin might explain the abrogation of the checkpoint arrest and could facilitate cytotoxic drug-damaged cells to undergo apoptosis. Furthermore, a recent study demonstrated that enzastaurin had a cooperative effect with gefitinib and was able to revert gefitinib resistance in cancer cells through the inhibition of Akt and VEGF pathways (Gelardi *et al*, 2008). These studies suggest that enzastaurin might be a promising novel agent in NSCLC patients.

Enzastaurin inhibited the downstream PKCβ signalling, PI3K/AKT pathway and the phosphorylation of glycogen synthase kinase-3β (Keyes *et al*, 2002; Graff *et al*, 2005). Anti-tumour and anti-angiogenic activity of enzastaurin was also demonstrated in tumour xenograft models, including NSCLC, and was confirmed using a standardised clonogenic assay in patient-derived tumour explants (Keyes *et al*, 2004). Significant reduction of VEGF protein levels following enzastaurin treatment, together with a significant decrease in intratumoural vessel density, has been demonstrated *in vivo* (Keyes *et al*, 2004). In the current study using a RTKs phosphorylation antibody array, we found elevated levels of VEGFR2 and VEGFR3 in the enzastaurin-sensitive cells. Our results are in agreement with previous data concerning enzastaurin and anti-angiogenic activity. These findings demonstrated that lung cancer cases with activated angiogenic activity should respond to enzastaurin treatment.

In this study, using gene-chip and pathway analysis, we identified 16 genes that correlated with sensitivity to enzastaurin. Pathway analysis also revealed that JAK1 was the most important molecule affected by enzastaurin treatment of NSCLC. The JAK is a non-RTK and can activate STAT3 transcriptional factor. The STAT3 is also persistently activated in about half of NSCLC tumours and is involved in tumour invasion, metastasis and angiogenesis through differential gene regulation (Haura *et al*, 2005; Song *et al*, 2011). Increased levels of JAK1 and STAT3 were observed in the sensitive cells in this study. Knockdown of JAK resulting in p-STAT3 also diminished the growth-inhibitory effect of enzastaurin in the sensitive cells. In contrast, overexpression of JAK1 by lentiviral-mediated production enhanced the drug sensitivity to enzastaurin in the sensitive cells. These results suggest that JAK expression levels can be used as predictive markers of enzastaurin sensitivity. Non-small-cell lung cancer patients with an activated JAK/STAT3 pathway are suitable cases for enzastaurin treatment.

MicroRNAs are small non-coding RNA molecules of about 20 nucleotides that are frequently located at chromosomal regions deleted or amplified in cancers, suggesting that miRNAs are a new class of genes involved in human tumourigenesis (Lu *et al*, 2005; Volinia *et al*, 2006; Yanaihara *et al*, 2006; Seike *et al*, 2009). Recently, miRNAs have been demonstrated as diagnostic and prognostic markers in lung cancer (Yanaihara *et al*, 2006; Seike *et al*, 2009). We previously reported that the inhibition of miR-21, whose upregulation is associated with EGFR mutations, can be a therapeutic strategy, either as a monotherapy or in combination with EGFR-TKI treatment (Seike *et al*, 2009). In this study, expression of miR-21 and its host gene, TMEM49, were significantly higher in enzastaurin-sensitive cells than in enzastaurin-resistant cells. In addition, a significant positive correlation was observed between miR-21 and JAK1. The STAT3 reportedly signals IL-6-induced upregulation of miR-21 in multiple myeloma cells (Löffler *et al*, 2007). We confirmed that JAK1 and its downstream target STAT3, containing three binding sites of miR-21 promoter, directly activated miR-21 in NSCLC cells. These results suggest that, in lung cancer, miR-21 affects the response to enzastaurin through the JAK/STAT signalling pathway.

In conclusion, we have identified unique molecules; genes, RTKs and miRNAs that are correlated with sensitivity to enzastaurin and have constructed an eight-gene signature to distinguish the sensitive cells from the resistant cells. Furthermore, we demonstrate that JAK1 is the most significant factor concerned in response to enzastaurin. Patient selection based on the JAK expression might be useful for future clinical development of enzastaurin therapy in NSCLC.

ACKNOWLEDGEMENTS

This study was supported in part by a Grant-in-Aid from the Ministry of Education, Culture, Sports, Science and Technology of Japan, and Basic and Clinical Studies on Functional RNA Molecules for Advanced Medical Technologies (to MS and AG).

Conflict of interest

The authors declare no conflict of interest.

Translational Therapeutics

REFERENCES

Barr LF, Campbell SE, Baylin SB (1997) Protein kinase C-beta inhibits cycling and decreases c-myc-induced apotosis in small cell lung cancer cells. *Cell Growth Differ* **8**: 381–392

Chiappori A, Bepler G, Barlesi F, Soria JC, Reck M, Bearz A, Barata F, Scagliotti G, Park K, Wagle A, Liepa AM, Zhao YD, Chouaki N, Iscoe N, von Pawel J (2010) Phase II, double-blinded, randomized study of enzastaurin plus pemetrexed as second-line therapy in patients with advanced non-small cell lung cancer. *J Thorac Oncol* 5(3): 369–375

Dreicer R, Garcia J, Hussain M, Rini B, Vogelzang N, Srinivas S, Somer B, Zhao YD, Kania M, Raghavan D (2010) Oral enzastaurin in prostate cancer: a two-cohort phase II trial in patients with PSA progression in the non-metastatic castrate state and following docetaxel-based chemotherapy for castrate metastatic disease. *Invest New Drugs* 29(6): 1441–1448

Faul MM, Gillig JR, Jirousek MR, Ballas LM, Schotten T, Kahl A, Mohr M (2003) Acyclic N-(azacycloalkyl) bisindolylmaleimides: isozyme selective inhibitors of PKCbeta. *Bioorg Med Chem Lett* 13(11): 1857–1859

Gelardi T, Caputo R, Damiano V, Daniele G, Pepe S, Ciardiello F, Lahn M, Bianco R, Tortora G (2008) Enzastaurin inhibits tumours sensitive and resistant to anti-EGFR drugs. *Br J Cancer* 99(3): 473–480

Gemma A, Li C, Sugiyama Y, Matsuda K, Seike Y, Kosaihira S, Minegishi Y, Noro R, Nara M, Seike M, Yoshimura A, Shionoya A, Kawakami A, Ogawa N, Uesaka H, Kudoh S (2006) Anticancer drug clustering in lung cancer based on gene expression profiles and sensitivity database. *BMC Cancer* **6**: 174

Glimelius B, Lahn M, Gawande S, Cleverly A, Darstein C, Musib L, Liu Y, Spindler KL, Frödin JE, Berglund A, Byström P, Qvortrup C, Jakobsen A, Pfeiffer P (2010) A window of opportunity phase II study of enzastaurin in chemonaive patients asymptomatic metastatic colorectal cancer. *Ann Oncol* 21(5): 1020–1026

Graff JR, McNulty AM, Hanna KR, Konicek BW, Lynch RL, Bailey SN, Banks C, Capen A, Goode R, Lewis JE, Sams L, Huss KL, Campbell RM, Iversen PW, Neubauer BL, Brown TJ, Musib L, Geeganage S, Thornton D (2005) The protein kinase Cbeta-selective inhibitor, Enzastaurin (LY317615.HCl), suppresses signaling through the AKT pathway, induces apoptosis, and suppresses growth of human colon cancer and glioblastoma xenografts. *Cancer Res* 65(16): 7462–7469

Haura EB, Zheng Z, Song L, Cantor A, Bepler G (2005) Activated epidermal growth factor receptor-Stat-3 signaling promotes tumor survival *in vivo* in non-small cell lung cancer. *Clin Cancer Res* 11(23): 8288–8294

Iliopoulos D, Jaeger SA, Hirsch HA, Bulyk ML, Struhl K (2010) STAT3 activation of miR-21 and miR-181b-1 via PTEN and CYLD are part of the epigenetic switch linking inflammation to cancer. *Mol Cell* 39(4): 493–506

Jemal A, Siegel R, Ward E, Hao Y, Xu J, Thun MJ (2009) Cancer statistics. *CA Cancer J Clin* 59: 225–249

Keyes K, Cox K, Treadway P, Mann L, Shih C, Faul MM, Teicher BA (2002) An *in vitro* tumor model: analysis of angiogenic factor expression after chemotherapy. *Cancer Res* 62(19): 5597–5602

Keyes KA, Mann L, Sherman M, Galbreath E, Schirtzinger L, Ballard D, Chen YF, Iversen P, Teicher BA (2004) LY317615 decreases plasma VEGF levels in human tumor xenograft-bearing mice. *Cancer Chemother Pharmacol* 53(2): 133–140

Körner A, Mudduluru G, Manegold C, Allgayer H (2010) Enzastaurin inhibits invasion and metastasis in lung cancer by diverse molecules. *Br J Cancer* 103(6): 802–811

Lahn M, McClelland P, Ballard D, Mintze K, Thornton D, Sandusky G (2006) Immunohistochemical detection of protein kinase C-beta (PKC-beta) in tumour specimens of patients with non-small cell lung cancer. *Histopathology* 49: 429–431

Li S, Phong M, Lahn M, Brail L, Sutton S, Lin BK, Thornton D, Liao B (2007) Retrospective analysis of protein kinase C-beta (PKC-β) expression in lymphoid malignancies and its association with survival in diffuse large B-cell lymphomas. *Biol Direct* 21: 2–8

Livneh E, Fishman DD (1997) Linking protein kinase C to cell-cycle control. *Eur J Biochem* 248(1): 1–9

Löffler D, Brocke-Heidrich K, Pfeifer G, Stocsits C, Hackermüller J, Kretzschmar AK, Burger R, Gramatzki M, Blumert C, Bauer K, Cvijic H, Ullmann AK, Stadler PF, Horn F (2007) Interleukin-6 dependent survival of multiple myeloma cells involves the Stat3-mediated induction of microRNA-21 through a highly conserved enhancer. *Blood* 110(4): 1330–1333

Lu J, Getz G, Miska EA, Alvarez-Saavedra E, Lamb J, Peck D, Sweet-Cordero A, Ebert BL, Mak RH, Ferrando AA, Downing JR, Jacks T, Horvitz HR, Golub TR (2005) MicroRNA expression profiles classify human cancers. *Nature* 435(7043): 834–838

Maemondo M, Inoue A, Kobayashi K, Sugawara S, Oizumi S, Isobe H, Gemma A, Harada M, Yoshizawa H, Kinoshita I, Fujita Y, Okinaga S, Hirano H, Yoshimori K, Harada T, Ogura T, Ando M, Miyazawa H, Tanaka T, Saijo Y, Hagiwara K, Morita S, Nukiwa T (2010) Gefitinib or chemotherapy for non-small-cell lung cancer with mutated EGFR. *N Engl J Med* 362(25): 2380–2388

Mina L, Krop I, Zon RT, Isakoff SJ, Schneider CJ, Yu M, Johnson C, Vaughn LG, Wang Y, Hristova-Kazmierski M, Shonukan OO, Sledge GW, Miller KD (2009) A phase II study of oral enzastaurin in patients with metastatic breast cancer previously treated with an anthracycline and a taxane containing regimen. *Invest New Drugs* 27: 565–570

Miyanaga A, Gemma A, Noro R, Kataoka K, Matsuda K, Nara M, Okano T, Seike M, Yoshimura A, Kawakami A, Uesaka H, Nakae H, Kudoh S (2008) Antitumor activity of histone deacetylase inhibitors in non-small cell lung cancer cells: development of a molecular predictive model. *Mol Cancer Ther* 7(7): 1923–1930

Mok TS, Wu YL, Thongprasert S, Yang CH, Chu DT, Saijo N, Sunpaweravong P, Han B, Margono B, Ichinose Y, Nishiwaki Y, Ohe Y, Yang JJ, Chewaskulyong B, Jiang H, Duffield EL, Watkins CL, Armour AA, Fukuoka M (2009) Gefitinib or carboplatin-paclitaxel in pulmonary adenocarcinoma. *N Engl J Med* **361**(10): 947–957

Morgillo F, Martinelli E, Troiani T, Laus G, Pepe S, Gridelli C, Ciardiello F (2008) Sequence-dependent, synergistic antiproliferatine and proapoptotic effects of the combination of cytotoxic drugs and enzastaurin, a protein kinase Cbeta inhibitor, in non-small cell lung cancer cells. *Mol Cancer Ther* **7**(6): 1698–1707

Mountain CF (1997) Revisions in the international system for staging lung cancer. *Chest* **111**: 1710–1717

Oh Y, Herbst RS, Burris H, Cleverly A, Musib L, Lahn M, Bepler G (2008) Enzastaurin, an oral serine/threonine kinase inhibitor, as second- or third-line therapy of non-small-cell lung cancer. *J Clin Oncol* **26**(7): 1135–1141

Ohe Y, Ohashi Y, Kubota K, Tamura T, Nakagawa K, Negoro S, Nishiwaki Y, Saijo N, Ariyoshi Y, Fukuoka M (2007) Randomized phase III study of cisplatin plus irinotecan versus carboplatin plus paclitaxel, cisplatin plus gemcitabine, and cisplatin plus vinorelbine for advanced non-small-cell lung cancer: Four-Arm Cooperative Study in Japan. *Ann Oncol* **18**(2): 317–323

Rademaker-Lakhai JM, Beerepoot LV, Mehra N, Radema SA, van Maanen R, Vermaat JS, Witteveen EO, Visseren-Grul CM, Musib L, Enas N, van Hal G, Beijnen JH, Schellens JH, Voest EE (2007) Phase I pharmacokinetic and pharmacodynamic study of the oral protein kinase C beta-inhibitor enzastaurin in combination with gemcitabine and cisplatin in patients with advanced cancer. *Clin Cancer Res* **13**: 4474–4481

Rascoe PA, Cao X, Daniel JC, Miller SD, Smythe WR (2005) Receptor tyrosine kinase and phosphoinositide-3 kinase signaling in malignant mesothelioma. *J Thorac Cardiovasc Surg* **130**(2): 393–400

Salgia R, Skarin AT (1998) Molecular abnormalities in lung cancer. *J Clin Oncol* **16**: 1207

Schiller JH, Harrington D, Belani CP, Langer C, Sandler A, Krook J, Zhu J, Johnson DH (2002) Comparison of four chemotherapy regimens for advanced non-small-cell lung cancer. *N Engl J Med* **346**: 92–98

Seike M, Goto A, Okano T, Bowman ED, Schetter AJ, Horikawa I, Mathe EA, Jen J, Yang P, Sugimura H, Gemma A, Kudoh S, Croce CM, Harris CC (2009) MiR-21 is an EGFR-regulated anti-apoptotic factor in lung cancer in never-smokers. *Proc Natl Acad Sci USA* **106**(29): 12085–12090

Shipp MA, Ross KN, Tamayo P, Weng AP, Kutok JL, Aguiar RC, Gaasenbeek M, Angelo M, Reich M, Pinkus GS, Ray TS, Koval MA, Last KW, Norton A, Lister TA, Mesirov J, Neuberg DS, Lander ES, Aster JC, Golub TR (2002) Diffuse large B-cell lymphoma outcome prediction by gene-expression profiling and supervised machine learning. *Nat Med* **8**(1): 68–74

Song L, Rawal B, Nemeth JA, Haura EB (2011) JAK1 activates STAT3 activity in non-small-cell lung cancer cells and IL-6 neutralizing antibodies can suppress JAK1-STAT3 signaling. *Mol Cancer Ther* **10**(3): 481–494

Tekle C, Giovannetti E, Sigmond J, Graff JR, Smid K, Peters GJ (2008) Molecular pathways involved in the synergistic interaction of the PKC beta inhibitor enzastaurin with the antifolate pemetrexed in non-small cell lung cancer cells. *Br J Cancer* **99**(5): 750–759

Vergote I, Amant F, Oskay-Oezcelik G, Musib L, Michel AL, Darstein C, Kania M, Bauknecht T, Sehouli J (2009) Carboplatin and paclitaxel in combination with oral enzastaurin in advanced ovarian or primary peritoneal cancer: results from a safety lead-in study. *Int J Gynecol Cancer* **19**(9): 1505–1510

Volinia S, Calin GA, Liu CG, Ambs S, Cimmino A, Petrocca F, Visone R, Iorio M, Roldo C, Ferracin M, Prueitt RL, Yanaihara N, Lanza G, Scarpa A, Vecchione A, Negrini M, Harris CC, Croce CM (2006) AmicroRNA expression signature of human solid tumors defines cancer gene targets. *Proc Natl Acad Sci USA* **103**(7): 2257–2261

Xia P, Aiello LP, Ishii H, Jiang ZY, Park DJ, Robinson GS, Takagi H, Newsome WP, Jirousek MR, King GL (1996) Characterization of vascular endothelial growth factor's effect on the activation of protein kinase C, its isoforms, and endothelial cell growth. *J Clin Invest* **98**(9): 2018–2026

Yanaihara N, Caplen N, Bowman E, Seike M, Kumamoto K, Yi M, Stephens RM, Okamoto A, Yokota J, Tanaka T, Calin GA, Liu CG, Croce CM, Harris CC (2006) Unique microRNA molecular profiles in lung cancer diagnosis and prognosis. *Cancer Cell* **9**(3): 189–198

Yoshiji H, Kuriyama S, Ways DK, Yoshii J, Miyamoto Y, Kawata M, Ikenaka Y, Tsujinoue H, Nakatani T, Shibuya M, Fukui H (1999) Protein kinase C lies on the signaling pathway for vascular endothelial growth factor-mediated tumor development and angiogenesis. *Cancer Res* **59**(17): 4413–4418

Zhang J, Anastasiadis PZ, Liu Y, Thompson EA, Fields AP (2004) Protein kinase C (PKC) betaII induces cell invasion through a Ras/Mek-, PKC iota/Rac1-dependent signaling pathway. *J Biol Chem* **279**(21): 22118–22123

BJC OPEN

British Journal of Cancer (2012) 106, 1953–1959

www.bjcancer.com

γ-Secretase inhibitor enhances antitumour effect of radiation in Notch-expressing lung cancer

H Mizugaki[1], J Sakakibara-Konishi*[,1], Y Ikezawa[1], J Kikuchi[1], E Kikuchi[1], S Oizumi[1], TP Dang[2] and M Nishimura[1]

[1]First Department of Medicine, Hokkaido University School of Medicine, North15, West7, Kita-ku, Sapporo 060-8638, Japan; [2]Department of Medicine, Division of Hematology/Oncology, University of Virginia, Charlottesville, VA, USA

BACKGROUND: Notch receptor has an important role in both development and cancer. We previously reported that inhibition of the Notch3 by γ-secretase inhibitor (GSI) induces apoptosis and suppresses tumour proliferation in non-small-cell lung cancer. Although radiation is reported to induce Notch activation, little is known about the relationship between radiation and Notch pathway.

METHODS: We examined the effect of combining GSI and radiation at different dosing in three Notch expressing lung cancer cell lines. The cytotoxic effect of GSI and radiation was evaluated using MTT assay and clonogenic assay *in vitro* and xenograft models. Expressions of Notch pathway, mitogen-activated protein kinase (MAPK) pathway and Bcl-2 family proteins were investigated using western blot analysis.

RESULTS: We discovered that the antitumour effect of combining GSI and radiation was dependent on treatment schedule. γ-Secretase inhibitor administration after radiation had the greatest growth inhibition of lung cancer *in vitro* and *in vivo*. We showed that the combination induced apoptosis of lung cancer cell lines through the regulation of MAPK and Bcl-2 family proteins. Furthermore, activation of Notch after radiation was ameliorated by GSI administration, suggesting that treatment with GSI prevents Notch-induced radiation resistance.

CONCLUSION: Notch has an important role in lung cancer. Treatment with GSI after radiation can significantly enhance radiation-mediated tumour cytotoxicity.

British Journal of Cancer (2012) **106,** 1953–1959. doi:10.1038/bjc.2012.178 www.bjcancer.com
Published online 17 May 2012

Keywords: Notch; γ-secretase inhibitor; radiation; apoptosis; non-small-cell lung cancer

Lung cancer is the most common cause of cancer related death in the world, and the incidence is still increasing. Although several therapies are available for advanced disease, they are palliative and the cure rate remains very low for patients. New therapeutic strategies are required to improve the poor prognosis of patients with non-small-cell lung cancer (NSCLC).

Notch receptor is a single-pass transmembrane protein, which regulates cell-fate determination in multi-cellular organisms. In mammals, there are four Notch receptors (Noch1–Notch4) and two families of ligands, Jagged (Jagged1 and -2) and Delta-like (Dll-1, -3 and -4) (Allenspach *et al*, 2002; Iso *et al*, 2003). Upon ligand binding, the Notch receptor undergoes a number of proteolytic cleavages. The final cleavage by the γ-secretase complex releases the Notch intracellular domain (NICD), which forms a nuclear complex with transcription factor CSL (CBF1, Sel, Lag-1) and induces expression of target genes, such as the Hairy and enhancer of split (*HES*) and Hairy/enhancer of split related with YRPW (*HEY*) gene family (Weinmaster and Kopan, 2006).

Several studies have highlighted the aberrant activation of Notch pathways in tumourigenesis of many cancers (Das *et al*, 2004; Curry *et al*, 2005; Duechler *et al*, 2005; Reedijk *et al*, 2005). We have demonstrated that Notch3 is expressed in ~40% of NSCLC tumours and that suppression of Notch3 by dominant negative or γ-secretase inhibitor (GSI) inhibits growth of lung cancer both *in vitro* and *in vivo* (Haruki *et al*, 2005; Konishi *et al*, 2007). γ-Secretase inhibitor modulates the Bcl-2 family proteins and downregulates MAPK pathway (Konishi *et al*, 2007). Our group also reported that Bim, BH3-only member of the Bcl-2 family proteins, is necessary for Notch3-dependent apoptosis and that the effect of Notch3 on Bim is through MAPK regulation (Konishi *et al*, 2010).

Although radiotherapy is routinely used to treat patients with lung cancer, resistance to radiation is one of the major reasons for radiotherapy failure in NSCLC. While many factors have been proven contributing to this observation, radiation has been shown to activate Notch in breast cancer and glioma. Given the role of Notch signalling in oncogenesis, these observations suggest that Notch represents a mechanism of radioresistance (Phillips *et al*, 2006; Wang *et al*, 2010).

In this study, we demonstrated the enhanced antitumour effect of GSI after radiation in Notch expressing lung cancer cell lines *in vitro* and *in vivo*. We also provide evidence that the observed antitumour effect involves Notch pathway. The mechanism involves apoptosis through the regulation of MAPK and Bcl-2 family proteins. Thus, our findings will help define a new strategy in modulating radiation therapy to enhance clinical efficacy in the treatment of patients with NSCLC.

MATERIALS AND METHODS

Cell lines and inhibitors

HCC2429 was established as previously described (Dang *et al*, 2000). The NSCLC cell lines, H460, A549 and H1395 were obtained

*Correspondence: J Sakakibara-Konishi; E-mail konishj@med.hokudai.ac.jp
Received 22 February 2012; revised 4 April 2012; accepted 11 April 2012; published online 17 May 2012

from American Type Culture Collection (Manassas, VA, USA). Cell lines were maintained in RPMI supplemented with 10% foetal calf serum at 37 °C in a humid environment in 5% CO_2. γ-Secretase inhibitor I (*in vitro*) and GSI XX (*in vitro, in vivo*) were obtained from Calbiochem (San Diego, CA, USA).

MTT proliferation assay

HCC2429 at 10 000 cells per well, H460 and H1395 at 500 cells per well were seeded into a 96-well plate and incubated overnight. HCC2429 and H460 were shown previously to have high Notch3 expression, whereas H1395 did not express Notch (Konishi *et al*, 2007). The cells were treated with GSI I and radiation simultaneously, radiation at 24 h after GSI I or GSI I at 24 h post-radiation. Treated cells were then incubated for 8 days. The MTT assay was performed to according to manufacturer's recommendation. The absorption was determined at 560 nm using the microplate reader (Varioskan Flash; Thermo Fisher Scientific, Lafayette, CO, USA).

Clonogenic assay

HCC2429 at 5000 cells per well, H460 and H1395 at 2000 cells per well were plated on 6-well plate and were then irradiated with 0 to 4 Gy as indicated after an overnight incubation. γ-Secretase inhibitor I at varying doses was added at 24 h after radiation and cells were incubated for 8 days. The cells were then fixed and stained for 1 min with 0.5% crystal violet in methanol. The number of colonies was counted manually. Survival fraction was calculated using the following formula: mean colony counts/cells inoculated × plating efficiency (PE). PE was defined as: mean colony counts/cells inoculated for unirradiated controls, as previously described (Cao *et al*, 2004).

Quantification of interaction of combination

Combination index (CI) for the GSI and radiation was described previously (Chou and Talalay, 1984; Gorodetsky *et al*, 1998). Accordingly, CI was calculated as follows:

$$CI = D/Dx + C/Cx + (D/Dx \times C/Cx). \quad (1)$$

Where Dx is the dose of radiation and Cx is the dose of GSI that yields a selected level of survival (x) when each agent is used alone. D is the dose of radiation and C is the dose of GSI that yields the same survival (x) when both treatments were combined. The level of survival selected to evaluate each set of combined treatments is lower than the survival following radiation alone. Combination index values are smaller than, equal to or greater than 1 represent supra-additive, additive and sub-additive effects of the combined treatment, respectively.

Apoptosis assays

HCC2429 and H460 were plated onto 6-well plates at the density of 1×10^6 cells per well and 3×10^5 cells per well respectively, incubated overnight, and subsequently treated with GSI I 1 μM for HCC2429 and 9 μM for H460 24 h after 8 Gy of radiation. HCC2429 and H460 were then incubated for 24 and 48 h, respectively. The cells were stained with FITC-conjugated Annexin V and propidium iodide (PI), using Annexin V-FITC Apoptosis Detection kit and according to manufacturer's recommendation (Calbiochem). The percentage of apoptotic cells was determined using a flow cytometry (BD FACSCalibur; Becton, Dickinson and Company, Franklin Lakes, NJ, USA).

Antibodies and western blot analysis

Notch3 was detected using a rabbit polyclonal antibody from Allele Biotechnology and Pharmaceuticals, Inc. (San Diego, CA, USA) at 1 : 500. Notch1 was detected using a mouse monoclonal antibody from Sigma-Aldrich Corp. (St Louis, MO, USA) at 1 : 500. The rabbit antibodies to HES1 and HEY1 were obtained from Santa Cruz Biotechnology, Inc. (Santa Cruz, CA, USA). The rabbit antibodies to Bcl-xL, phosphor-Bcl-2 (p-Bcl-2), Bcl-2, extracellular signal-regulated kinase (ERK), p-ERK, AKT, p-AKT and poly (ADP-ribose) polymerase (PARP) were obtained from Cell Signaling Technology, Inc. (Danvers, MA, USA). Bim antibody was obtained from Sigma-Aldrich Corp. The band intensity was demonstrated by quantitative densitometric analysis using NIH Image Ver1.62 software (NIH, Bethesda, MD, USA). Standardisation was performed with actin measured in the same blots with anti-actin antibody (A-2066, Sigma-Aldrich Corp.). Quantifications were shown by the ratios of treated protein expression/untreated protein expression.

In vivo tumourigenicity

All animal husbandry and experiments were performed under a protocol approved by Institutional Animal Care Committee at Hokkaido University School of Medicine. H460 and A549 at 1.0×10^6 cells were diluted in 100 μl of PBS and injected subcutaneously into right posterior legs of athymic, 5-week-old, female nude mice (*nu*+/*nu*+). When the tumours were palpable, the mice were randomly assigned to the radiation group, the GSI group, the combination group or the control group. Each group consisted of five mice. The mice in the radiation alone group received 8 Gy of radiation at day 1 and 8. The radiation was administered to the tumour with the remainder of the body shielded with lead. In the GSI group, 200 $\mu g\,kg^{-1}$ GSI XX was administered by i.p. at day 2, 3, 4 and 9, 10, 11, as previously described (Tanaka *et al*, 2009; Konishi *et al*, 2010). The combination group received both GSI XX and radiation in similar schedule. The tumours were then measured every 2 days using a digital caliper. Tumour volume (TV) was determined using the formula: TV = (Length) × (Width) × (Height)/2 (Cao *et al*, 2004). Tumour growth rate (%TV) on day X was calculated as: (TV on day X/TV on day1) × 100, as previously described (Konishi *et al*, 2010). Some tumours were resected on day 15 and the expression of NICD3 was determined by western blot analysis.

Statistical analysis

Determination of significance between the control and observation arms of both *in vitro* and *in vivo* assays was analysed using the non-parametric Mann–Whitney U test. Statistical significance was established at the P value < 0.05. Calculations were performed using SPSS, version 11.0.1 (SPSS Inc., Chicago, IL, USA).

RESULTS

Treatment with GSI at 24 h after radiation enhanced growth inhibition of lung cancer *in vitro*

To determine whether the combining GSI and radiation can inhibit lung cancer proliferation, we treated Notch expressing lung cancer cell lines, HCC2429 and H460 with increasing dose of GSI and radiation. Cell viability of both cell lines was determined using the MTT assay. Neither concurrent treatment schedule nor radiation after GSI I administration had a significant impact on tumour proliferation compared with single treatment with GSI I alone (0 Gy) (Figure 1A). In contrast, when GSI I was administrated after radiation, there was a significant decrease in IC_{50} of GSI I compared to treatment with GSI I alone (0 Gy) in HCC2429 and H460 (Figure 1B and Supplementary Table 1). Clonogenic assay was performed to confirm the results of the MTT assay. This treatment schedule resulted in greater suppression in colony formations compared with radiation alone (Figure 1C). On the other hand, in H1395, which does not express Notch, no difference

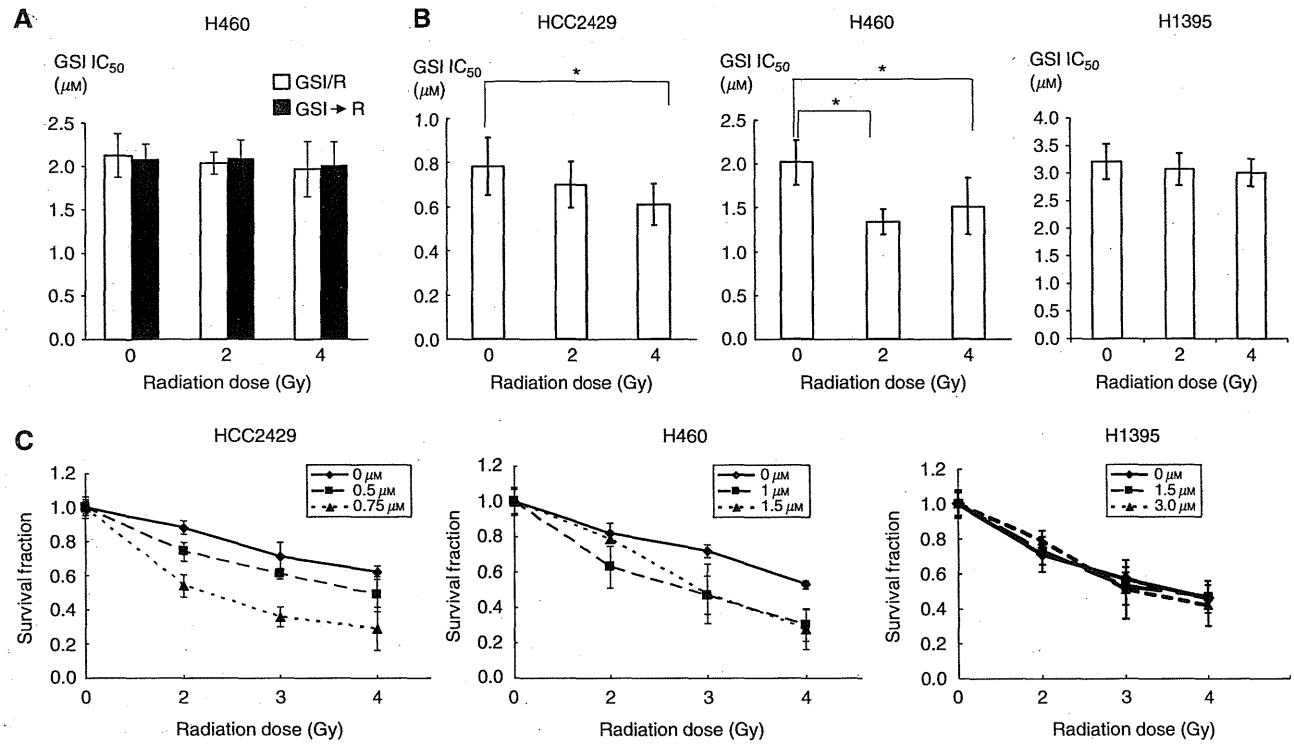

Figure 1 GSI after radiation suppressed proliferation of lung cancer. (**A**) Comparison of IC_{50} values in the different treatment schedule in the MTT proliferation assay. Neither concurrent treatment schedule nor radiation after GSI I administration had a significant impact on tumour proliferation compared with GSI I alone (0 Gy). Plated cells were treated with GSI I and radiation simultaneously or radiation at 24 h after GSI I administration ($n = 5$). Treated cells were incubated for 8 days. GSI/R: concurrent treatment schedule. GSI→R: radiation after GSI I administration. (**B**) Comparison of IC_{50} in GSI I after radiation. Plated cells were treated with GSI I at varying doses at 24 h after radiation. IC_{50} was less for combined therapy than for GSI I alone in both HCC2429 and H460 cell lines ($n = 5$). $^*P < 0.05$. On the contrary, IC_{50} was not different between GSI alone and combination in H1395. (**C**) GSI I after radiation decreased clonogenic survival in HCC2429 and H460, but not in H1395 ($n = 3$). Cells were plated overnight and then exposed to radiation with 0 to 4 Gy as indicated. GSI I at varying doses was added at 24 h after radiation and then cells were incubated for 8 days.

Table 1 Combination index (CI) with respect to survival fraction of HCC2429 and H460 cells exposed to GSI I after radiation

HCC2429				H460			
Survival fraction (%)	Radiation (D^a) (Gy)	GSI (C^a) μM	CI^b	Survival fraction (%)	Radiation (D^a) (Gy)	GSI (C^a) μM	CI^b
50	2.0	0.47	0.96	50	2.0	1.29	0.93
50	3.0	0.28	1.00	50	3.0	0.98	1.00
50	4.0	0.20	1.10	50	4.0	0.68	1.21
25	2.0	0.56	0.78	25	2.0	1.64	0.83
25	3.0	0.45	0.86	25	3.0	1.56	0.99
25	4.0	0.31	0.87	25	4.0	1.46	1.10
10	2.0	0.66	0.66	10	2.0	2.43	0.84
10	3.0	0.65	0.76	10	3.0	2.26	0.91
10	4.0	0.64	0.86	10	4.0	1.98	0.94

Abbreviations: CI = combination index; GSI = γ-secretase inhibitor. [a]C and D were obtained from the survival fraction curve (Figure 1C). [b]CI was calculated for different levels of survival fraction according to Equation 1.

between single treatment and combination was observed in IC_{50} and colony formations (Figure 1B and C and Supplementary Table 1), suggesting that combination is only effective in Notch expressing cell lines. By determining the CI values of GSI I after radiation in HCC2429 and H460, we noted supra-additive or additive effects of combination in the most set of combining treatment (Table 1). Therefore, this sequential treatment schedule was employed in all of the following experiments.

GSI prevents radiation-dependent Notch activation

When HCC2429 and H460 were treated with GSI I alone, the expression of NICD in both cell lines was decreased in a dose-dependent manner (Figure 2A). To investigate the effect of radiation on Notch pathway, the expressions of NICD1, NICD3 and target genes, *HES1* and *HEY1* were assessed after cells were irradiated at 2 and 4 Gy, respectively. In HCC2429, the expression of NICD1 was upregulated at 24 h after radiation and this upregulation was observed up to 48 h following radiation, whereas the expression of NICD3 was unchanged. Notch1 mRNA was also upregulated after radiation, suggesting that radiation induces transcripts of Notch1 (Supplementary Figure 1). In H460, in which the baseline expression of Notch3 level is lower, NICD3 expression was increased at 24 and 48 h after radiation and the expression of NICD1 was not induced by radiation (Figure 2B). Notch3 mRNA was upregulated after radiation in H460 (Supplementary Figure 1). HEY1 expression was upregulated in both cell lines at 48 h after radiation compared with control. Then, we examined NICD1 and NICD3 expression when cells were treated with GSI I, radiation or the combination treatment. Radiation-induced NICD1 upregulation was ameliorated by the combination in HCC2429. Radiation-induced NICD3 enhancement was also reduced by the combination in H460 (Figure 2C).

Addition of GSI enhances radiation-induced apoptosis

To examine whether addition of GSI following radiation can induce apoptosis compared either treatment alone, we treated HCC2429 and H460 with GSI I after radiation and determined the proportion of apoptotic cells using Annexin V and PI and flow